Marine Biology 117, 1–22 (1993)

Marine Biology
International Journal on Life in Oceans and Coastal Waters

Highly directional swimming by scalloped hammerhead sharks, *Sphyrna lewini*, and subsurface irradiance, temperature, bathymetry, and geomagnetic field

A. P. Klimley

Bodega Marine Laboratory, University of California at Davis, P.O. Box 247, Bodega Bay, California 94923, USA

Received: 24 February 1993 / Accepted: 6 May 1993

Abstract. The homing behavior of scalloped hammerhead sharks (*Sphyrna lewini*) to and fro between Espiritu Santo Seamount and Las Animas Island and the surrounding pelagic environment was studied to reveal their mechanisms of navigation in the oceanic environment. Four sharks were tagged with ultrasonic transmitters and tracked at the former location and one shark at the latter site during July, August, or September between 1981 and 1988. Hammerhead swimming movements were highly oriented: the mean coefficient of concentration (r) for sets of ten consecutive swimming directions recorded during eight homing movements by three hammerhead sharks ranged from 0.885 to 0.996. Drift within a current could not explain this directionality, since highly variable directions were recorded from a transmitter floating at the sea surface after becoming detached from a shark. Forward swimming momentum was an unlikely explanation, since highly directional swimming was maintained for a period of 32 min with only a gradual change in course. To maintain directionality over this period, an environmental property should be necessary for guidance. The hammerheads swam at night, with repeated vertical excursions ranging from 100 to 450 m deep, out of view of either the sea surface or the sea floor. The sharks' vertical diving movements were compared to distributions of spectral irradiance (relative to elasmobranch scotopic and photopic visual sensitivities), temperature, and current-flow directions in the water column. No relationships were evident between these properties and the sharks' oriented swimming movements. Movements of scalloped hammerhead sharks to and from a seamount were compared to topographic features in bathymetry and geomagnetic field leading away from the seamount. Sharks swam repeatedly over fixed geographic paths, and these paths occurred less often along submarine ridges and valleys than maxima and minima in the geomagnetic field. No significant difference existed between the degree of association of points from the sharks' tracks and points from track simulations and $\geq 20°$ changes in the slope of the depth record. On the other hand, significantly more points from the sharks' tracks were associated with slope changes in the magnetic intensity record than points from track simulations. A magnetic intensity gradient of 0.037 nanoteslas/m (nT/m) existed at 175 m depth, where a shark swam directionally, and this gradient was three times steeper than that measured at the sea surface and exceeded that recorded at a depth of 200 m. The hammerheads are hypothesized to find the seamount using geomagnetic topotaxis. The shark could be attracted to and move back and forth along ridges and valleys, features in the relief of magnetic field intensities occurring over a geographical area.

Introduction

Although few would question that the easily observed flight of migratory birds is highly oriented, no such consensus of opinion exists on the degree of directionality to swimming by migratory fishes. Saila and Shappy (1963) argued that adult salmon could return to their natal streams by simply moving in steps of random directions and lengths with only a slight directional bias based upon an external reference such as the sun. However, Quinn and Groot (1984) found that salmon arrived at the streams earlier than expected based upon the speeds and travel distances used in the simulation model of Saila and Shappy. These shorter periods of transit could result if the salmon swam in a highly oriented manner. However, neither homing mechanism has been evaluated by tracking salmon in the ocean distant from the coast. In the absence of knowledge of the movements of salmon, the component of randomness has been adjusted in subsequent models to obtain better consistency between speed of swimming, travel distance, and arrival time of salmon at the natal stream (Bovet and Benhamou 1988, Hiramatsu and Ishida 1989, Jamon 1990).

Salmon tracked by means of ultrasonic telemetry in coastal estuaries and other species tracked in the oceanic environment do swim at times in straight paths. The tracks of these fishes consist of point-to-point move-

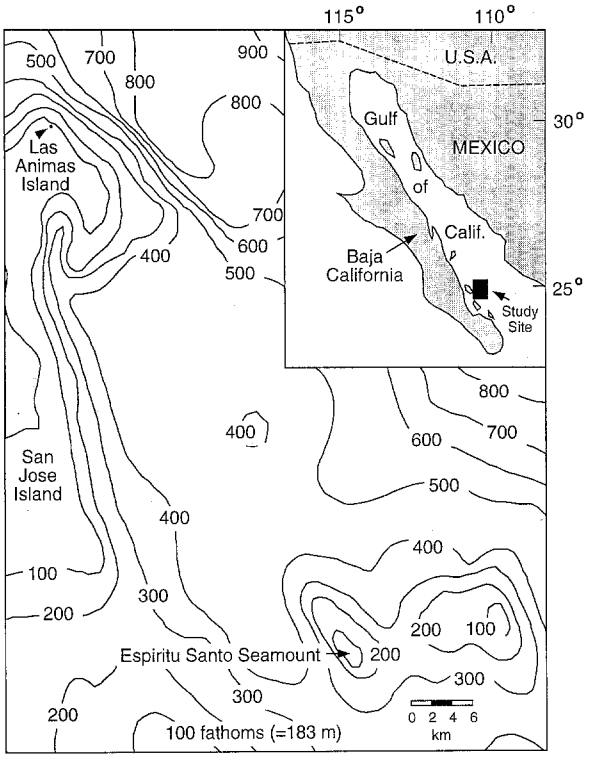

Fig. 1. Study area in Gulf of California. The two sites where *Sphyrna lewini* were tracked were Espiritu Santo Seamount and Las Animas Island

ments, indicated by vectors (or arrows) drawn from one position of the fish to the next, determined after intervals of 15 to 30 min. The directions of the movements of Atlantic and sockeye salmon (*Salmo salar* and *Oncorhynchus nerka*), scalloped hammerhead sharks (*Sphyrna lewini*) and blue sharks (*Prionace glauca*) cluster in a single direction (Westerberg 1982a, Klimley and Nelson 1984, Landesman 1984, Quinn et al. 1989, Carey and Scharold 1990). However, non-uniform distributions of these directions could result, were the fishes to remain motionless and drift in a current with a constant flow direction. The tracks of striped marlin (*Tetrapturus audax*) are composed of straight-line movements over ground, yet their general heading changes when the ocean current shifts direction (R. Brill et al. personal communication). This relationship implies that directionality of these movements results partly from drifting of the marlin in ocean currents. Unequivocal demonstration that a fish actively orients requires direct measurement of the directions of its swimming motions. These directions have only been recorded for the plaice *Pleuronectes platessa*, using a low-resolution sensor with only eight compass sectors (Greer Walker et al. 1978, Harden Jones 1981, Harden Jones and Arnold 1982). The headings of plaice were highly oriented during excursions (one lasting 14 min) away from the bottom which could not, therefore, serve as a visual reference.

Directionality to either the point-to-point movements or swimming motions of fishes in the ocean suggests the importance of an environmental property for guidance. Observations of straight-line flight by birds led to the investigation of the guiding effect of topography, the sun and stars, and the earth's main geomagnetic field (see review by Walcott and Lednor 1983). Similar orientation in fishes also indicates the existence of a guiding feature, although the different nature of the oceanic environment may necessitate the use of different receptors and environmental properties for guidance.

The homing behavior of the scalloped hammerhead shark is an ideal response for the study of the mechanism of navigation in the oceanic environment. These sharks swim in schools at seamounts and islands during the daytime (Klimley 1985). Individuals leave at dusk to forage in the surrounding pelagic environment and return by dawn on the following morning (Klimley and Nelson 1984, Klimley 1987, Klimley et al. 1988). The point-to-point movements comprising the nocturnal movements are highly oriented (Klimley and Nelson 1984), suggesting the use of an environmental property for guidance.

In the present study, the degree of directionality to the swimming of scalloped hammerheads is described during homing movements to Espiritu Santo Seamount and Las Animas Island in the Gulf of California (Fig. 1). Secondly, the vertical excursions of these hammerheads are compared to the distributions of irradiance, temperature, and current direction in the water column. Thirdly, the paths of the hammerheads are compared to the locations of topographic features (ridges and valleys or maxima and minima) in the seafloor and geomagnetic field. The potential of each environmental property is evaluated for its usefulness in guiding the homing sharks back to the two sites.

Materials and methods

Tracking

Four scalloped hammerhed sharks (*Sphyrna lewini*) were tagged with ultrasonic telemetry transmitters and tracked at Espiritu Santo Seamount, and a single hammerhead shark was tagged and tracked at Las Animas Island. The telemetry studies were conducted during cruises aboard the R. V. "Juan de Dios Batiz" and "Robert Gordon Sproul" during July, August, and September of 1981, 1986, and 1988. Each shark was tagged as follows. Carrying a transmitter mounted on a pole spear, the author made a breath-hold dive into a school of hammerhead sharks. The tag was then attached to an individual between its first and second dorsal fins by inserting a dart into the shark's musculature with a monofilament line leading to the transmitter. Because the tags were slightly buoyant, they floated just above the shark's dorsum and were observed to remain closely aligned with the body axis of the shark.

The position of each tagged shark was determined at 15 min intervals by one of two methods. Most positions were plotted from a radar bearing and range from the large research vessel to a small launch (which was situated above the tagged shark) and another bearing and range from the research vessel to a radar reflector on a balloon attached to a buoy moored at the seamount. Some of the shark positions were based upon a radar bearing and range from the research vessel to the launch, and latitudinal and longitudinal coordinates of the vessel obtained from the Global Positioning System (GPS). The spatial error of the radar-determined positions, which comprised most of the tracks, was established from the separation between radar and GPS-determined positions of the large vessel. The spatial accuracy of GPS positions, triangulated from four or more satellites, was 10 m (Hurn 1989). The median, 75th percentile, and range of positional error was calculated from ten paired measurements at each of five distances from the seamount (Table 1).

Table 1. Median, 75th percentile (75th perc.), and range of positional error at five distances (Dist.) from Espiritu Santo Seamount. Error was based upon spatial separation between paired radar and Global Positioning System determined positions

Dist. (km)	(*N*)	Median (±km)	75th perc. (+km)	Range (±km)
2	(10)	0.106	0.131	0.323
6	(10)	0.245	0.245	0.415
10	(10)	0.318	0.383	0.561
14	(10)	0.371	0.416	0.654
18	(10)	0.334	0.526	1.047

Behavioral and environmental measurements

Sensors on each transmitter recorded the swimming direction and depth of the shark as well as the level of light and temperature of the water adjacent to the shark. The transmitter's signal was detected with an omnidirectional hydrophone leading to an ultrasonic receiver (Ultrasonic Telemetry Systems, MR32-1). The magnitude of the property recorded by a sensor was proportional to the length of interval between successive ultrasonic pulses. Each sensor was interrogated and the serial order of the five sensors was repeated again and again. A laptop computer (Zenith, Z-171) and electronic interface (see Cigas and Klimley 1987) timed the intervals and converted these to the behavioral and environmental measurements by interpolation from calibration files stored on disk consisting of arrays of pulse intervals of increasing length and the corresponding directions, depths, irradiance levels and temperatures, measured in the laboratory.

One aim of this study was to determine whether a tagged shark swam selectively at depths where one environmental property was present and others were absent. This would imply that one specific property was useful in guiding the shark's movement. For this reason, irradiance levels, water temperature and current direction were recorded at 25 m intervals by sensors on a second ultrasonic telemetry transmitter that was repeatedly lowered to a 200 m depth from a second launch positioned near the shark. This transmitter was mounted on a vane which oriented in the direction of current flow. The second launch carried another receiver, electronic interface, and microcomputer for recording environmental measurements. The flow of water at the surface with respect to the bottom was determined at hourly intervals from the change in position of a drifter allowed to float at the surface for 15 min. This unit consisted of a rectangular polyethylene sheet (2 × 3 m) which extended downward below a donut-shaped float.

Klimley and Nelson (1984) previously reported that scalloped hammerheads make highly directional point-to-point movements. To assess the directionality of swimming by the hammerheads, it was necessary to utilize a sensor with greater resolution and accuracy than the sensor used by Greer Walker et al. (1978) in their studies on plaice. Their sensor detected whether a heading was within one of eight 45° sectors comprising the compass rose (see Mitson et al. 1982). The sensor used in this study had a resolution of ±1°, an accuracy of ±3°, and precision of ±1°.

The light level perceived by the shark was measured with sensors designed to emulate the visual capabilities of elasmobranchs. Each sensor was located on the side of the transmitter in a position similar to the location of a hammerhead's eyes on either end of its laterally elongated rostrum. Sharks have both photopic and scotopic vision (Gruber and Cohen 1978). Photopic vision is the ability to discriminate intensity changes when the eye is adapted to bright light. Scotopic vision is the ability to detect minute levels of light after the eye is adapted to darkness. These differences are attributed to the presence of cone and rod receptors in the shark's retina, each having different light-sensing capabilities. The cones are less sensitive to light than the rods. Furthermore, cone receptors are most sensitive to wavelengths in the green region of the irradiance spectrum while rods are most sensitive to wavelengths in the blue-green region. A photopic sensor was made from a photocell with a linear response to fluctuations in brightness at higher levels and this photocell was covered with a different filter which allowed only green irradiance to pass. A scotopic sensor was fabricated from a photocell with a large and linear response to minute brightness changes at low levels of irradiance. This photocell was covered by a filter which permitted only blue-green irradiance to pass. The magnitude of measurements from the photopic and scotopic sensors differed for the same broadband irradiance conditions. The photopic sensor recorded intensity changes during the bright-light conditions of day. The scotopic sensor detected the presence of extremely dim light during nighttime.

Bathymetric and magnetic surveys

Bathymetric and magnetic surveys were carried out to compare the paths taken by the sharks to and from the seamount to the locations of ridges and valleys in seafloor topography or maxima and minima in the local magnetic field which led away from the seamount.

Traces of bottom depth and total magnetic field intensity were recorded continuously on a sonar and magnetometer while the research vessel traveled at a constant speed of 8 knots through 12 concentric circles, each separated by 1.85 km (1.0 nautical mile) around the seamount (four nearest circles illustrated in Fig. 2A). Concentric, rather than parallel, survey lines were made because a more regular survey path resulted from steering the vessel with a constant rudder angle while using the ship's radar to maintain a constant distance between the ship and the seamount. The position of the vessel was determined at 0.93 km (0.5 nautical mile) intervals along the survey path. The sonar (Gifft GDR, 12 kHz) recorded depth at a rate of one measurement per sec with 1.0 m resolution. Each depth record corresponds to one clockwise movement of the sonar around the seamount. Fig. 2B shows the record from the circular path second nearest to the seamount. The marks on the abscissa represent those points where the vessel's position was determined. A proton precession magnetometer (EG & G Geometrics, Model G-811) recorded total magnetic field intensity at a rate of one measurement per second with 0.5 nT resolution on a 50 nT scale. If the magnetic intensity increased continuously, the trace rose from the bottom of the chart until it reached the top and then began to rise again from the bottom (Fig. 2C). Measurements of bottom depth and magnetic intensity and the corresponding geographic coordinates were later entered into a mapping program (MacGridzo) on a Macintosh IIx computer to produce 3-D bathymetric and geomagnetic contour maps based upon the inverse square gridding algorithm.

Because field measurements were made over a period of 4 d, it was necessary to remove from the data any changes in the earth's magnetic field due to diel and seasonal fluctuations (see Skiles 1985). Both within-day (ca. 50 nT) and between-day (8 nT) variations were removed from the intensity measurements at the control points in the following manner. Each time a measurement was obtained for a station in the survey area, a corresponding intensity measurement was recorded at a fixed site on Espiritu Santo Island, along the edge of the survey area less than 20 km from the seamount. The ship-based measurements were normalized with respect to a single measurement recorded at 20.00 hrs on the island, when both the point-to-point movements and telemetered swimming directions from Shark A were highly oriented. This was accomplished by adding or subtracting from the intensity measurement from each position along the survey path the differences between the intensity simultaneously recorded at the stationary site and the intensity measured there at 20.00 hrs on that day. The mathematical operation depended upon whether the former measurement at the stationary site was less or greater than the intensity recorded at 20.00 hrs. Between-day variability was removed by calculating mean intensities over each 24 h period and all measurements on each successive day to those of Day 1.

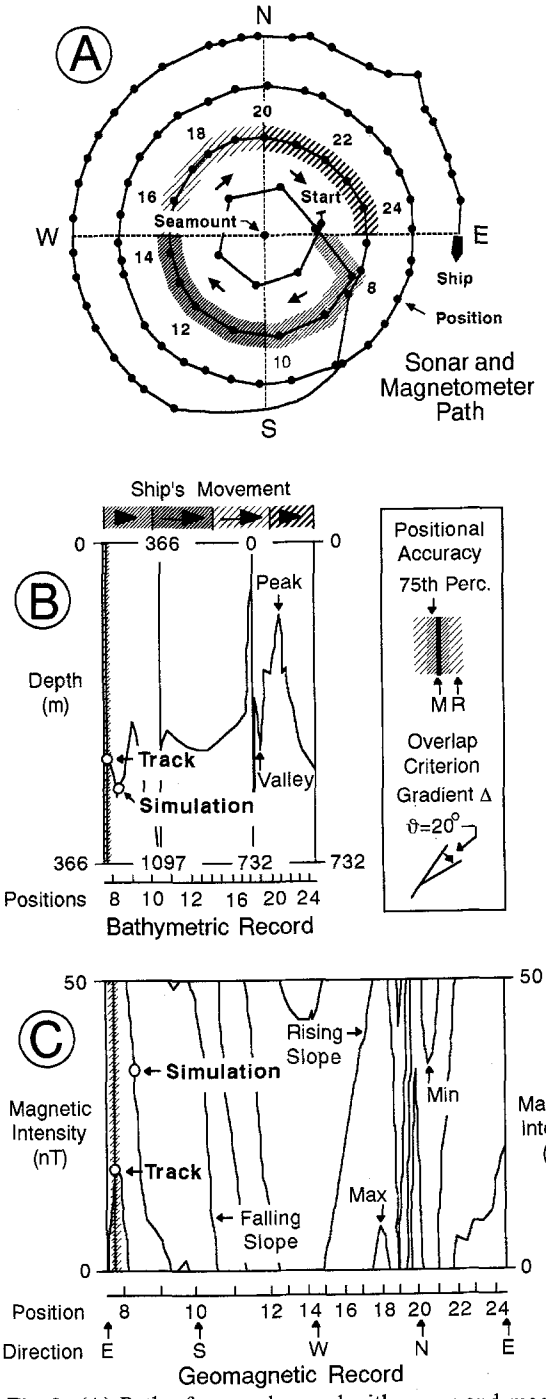

Fig. 2. (A) Path of research vessel with sonar and magnetometer; circles and numbers indicate vessel positions; shades of hatching distinguish quadrants of magnetometer path; arrows indicate direction of ship's movement in (B); only 4 of 12 concentrically circular survey tracks are shown. (B) Depth trace recorded as vessel moved along circular path second nearest to seamount (see Fig. 2A); numbers and marks on abscissa are positions shown in (A); arrows above record indicate direction of vessel's movement; median (M), 75th percentile, and range (R) of positional accuracy shown on right. (C) Trace of total magnetic intensity recorded as magnetometer was towed around path

Contour maps only approximate the relief of the bottom or geomagnetic field from measurements at a specified number of fixed positions using a mapping algorithm within the computer program. More accurate comparisons of hammerhead movements to the above two properties were achieved by determining those points on the sonar and magnetometer record where the vessel passed over

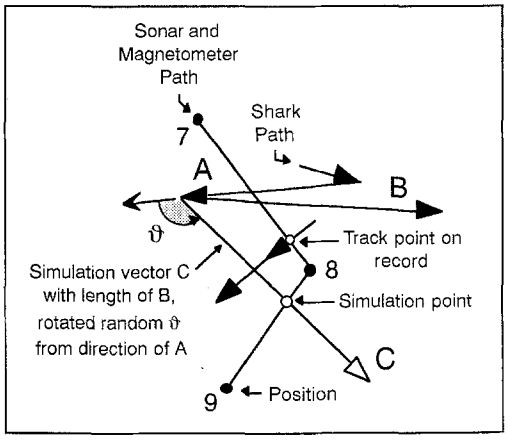

Fig. 3. Points (o) on both sonar and magnetometer records (data points labelled "Track" and "Simulation" in Fig. 2B, C) where survey path intersected actual tracks of *Sphyrna lewini* (black arrows) and track simulations (open arrows). Simulation vector was generated for each vector in track, e.g. Simulation Vector C had an identical length to Track Vector B but a random amount of rotation away from direction of previous Track Vector A

paths of sharks (data points marked "Track" and "Simulation" in Fig. 2B, C). This was accomplished by measuring the distance between two successive positions on the survey path, the one immediately before and after the magnetometer crossed the path of the homing shark, and the distance between the initial position and the point of intersection with the shark's track. A fraction, consisting of the latter value divided by the former, was multiplied by the distance between the corresponding marks on the bathymetric and geomagnetic records. The point of intersection with the shark's path occurred at this distance from the first mark. For contrast with the points from the shark's path, additional points were determined on the sonar and magnetometer records for simulated vectors, slightly different from those comprising the track of the shark. For example, a Simulation C was generated for Vector B of the track by rotating another vector with the length of B a random distance away from the direction of A, the vector immediately preceding B (Fig. 3). The rotations were randomized by choosing integers from a random-number table (see Table D in Rohlf and Sokal 1969) and converting these integers to angles using the mathematical operation modulus. The points of intersection of the simulated vector with sonar and magnetometer paths (open data points in Fig. 3) were then found on the bathymetric and magnetic records (Fig. 2B, C).

In order to determine the magnetic gradient experienced by an orienting shark, another proton precession magnetometer (EG & G Geometrics, G-866) was lowered at two stations on either side of the path of Shark A when this exhibited highly oriented headings. The total magnetic field intensity was recorded at 25 m intervals to a depth of 200 m. A gradient (in nT/m) was calculated for each depth from the difference between the intensities measured at the two stations divided by distance between the two stations. The resulting gradients were plotted as a function of depth.

Statistical analysis

The sharks might swim along ridges or valleys in the bottom topography. These are apparent as peaks and valleys in the trace of bottom depth. Alternatively, the sharks might move along maxima or minima in the magnetic field. The latter are boundaries to different magnetic gradients, characterized by different rates of change in magnetic intensity encountered when moving in a particular direction due to a change in the degree of magnetization of the seafloor. On a 3-D contour map, the strength of a gradient was proportional to the steepness of slope of the surface. A gradient boundary existed where the slope of the surface of intensities changed to form a maximum (ridge) minimum (valley). On the magnetometer record,

the gradient was proportional to the steepness of the trace because the magnetometer was dragged across the bottom at a constant speed of 11.1 km/h (= 6.0 nautical miles/h) (Fig. 2C). The intensity trace rose in a direction to the right of the record when the magnetometer was towed over the seafloor with increasing degrees of magnetization, and the trace then dropped as the magnetometer passed over ground with decreasing levels of magnetization. This resulted in a maximum in the record. Conversely, if the direction of movement by the magnetometer was reversed relative to the increasing and decreasing gradients of magnetization, a minimum was recorded on the trace of the geomagnetic record.

If sharks swam along ridges and valleys on the seafloor or maxima and minima in the magnetic field leading away from the seamount, the shark positions should be clustered at peaks and valleys in the depth record (Fig. 2B) or maxima and minima in the magnetic record (Fig. 2C). However, two changing geomagnetic gradients could occur if the ridge were flattened at the top or if the bottom of the valley were wide. Shark positions might also be clustered at these points. In fact, shark positions might be expected to be common anywhere the rising or falling intensity trace flattened temporarily before continuing with the same slope. An objective yet general definition of a slope or gradient boundary was used for the statistical comparisons: a $\geq 20°$ angular change in the slope of the trace of the record (see overlap criterion in Fig. 2B). The association of the shark with the slope discontinuity was based upon the overlap of bands indicating the degree of spatial accuracy associated with the point showing the shark's position and that of the nearest 20° change in trace slope on the record. The three levels of accuracy used in such comparisons were the median, 75th percentile, and range (Fig. 2B, C).

Results

Highly directional swimming

Highly directional swimming was recorded for all *Sphyrna lewini* tracked during nocturnal excursions away from the schooling sites of Espiritu Santo Seamount and Las Animas Island into the surrounding pelagic environment and back to these locations. Coefficients of concentration (for definition see Zar 1974) were calculated for sets of ten consecutive swimming directions from eight homing movements of three sharks (Table 2). The high degree of swimming directionality was apparent from coefficients of 0.999 which were recorded during four of the eight homing movements (A1, B1, C2 and C3). The sharks swam directionally throughout their excursions: the mean r calculated from all sets of directional measurements recorded per track exceeded 0.900 during five of the eight homing movements (A1, C1, C3, C4, C5). This directionality is apparent from the clusters of arrows which indicate the shark's constant heading (i.e., bearing) in the circular diagrams of swimming directions recorded at points along the track of Shark A at the seamount (Fig. 4) and along Tracks 1 and 2 of Shark E at the seamount (Fig. 5). Even when farthest from their home sites, both sharks swam highly directionally. The coefficient r for swimming directions (SD) recorded during the point-to-point movement of Shark A 19 km from the seamount was 0.998 (SD5, Fig. 4), and the coefficient recorded during a movement of Shark E 13 km from the island was 0.990 (SD4, Fig. 5).

Passive transport vs active orientation

Passive transport of sharks by water currents did not explain the directionality of the sharks' movements. The distances floated by drifters deployed near Shark E were

Table 2. *Sphyrna lewini.* Size and sex of Hammerheads A–E and distances (Dist.) moved from Espiritu Santo Seamount and Las Animas Island during homing movements. Maximum, mean, and minimum coefficients of concentration (r) are given for N sets of ten consecutive swimming directions recorded during each movement. Same measures are given for Track F1 of transmitter from Shark C after this had become detached after Homing Movement C6 and had floated to the surface

Location	Length (cm)	Sex (M/F)	Homing movement	Date	Dist. (km)	Sets (N)	r		
							max.	mean	min
Espiritu Santo Seamount									
Shark A	200	F	A1	8–9 Aug. 1986	19.4	(6)	0.999	0.955	0.900
Shark B	175	F	B1	23–24 July 1989	8.9	(–)	–	–	–
			B2	24–25 July 1989	20.2	(–)	–	–	–
			B3	25–26 July 1989	7.2	(–)	–	–	–
			B4	27–28 July 1989	13.5	(–)	–	–	–
			B5	28–29 July 1989	11.6	(–)	–	–	–
			B6	29–30 July 1989	11.9	(–)	–	–	–
			B7	30–31 July 1989	11.5	(–)	–	–	–
Shark C	225	F	C1	5 Aug. 1989	2.1	(4)	0.961	0.942	0.911
			C2	5–6 Aug. 1989	7.8	(7)	0.999	0.888	0.669
			C3	6 Aug. 1989	2.9	(4)	0.999	0.996	0.986
			C4	6–7 Aug. 1989	4.4	(7)	0.994	0.911	0.656
			C5	7 Aug. 1989	8.4	(–)	–	–	–
			C6	7–8 Aug. 1989	8.9	(6)	0.997	0.949	0.892
Shark D	175	F	D1	15–16 July 1981	17.1	(–)	–	–	–
Las Animas Island									
Shark E	125	F	E1	29 July 1988	12.3	(7)	0.999	0.885	0.543
			E2	30 July 1988	3.3	(2)	0.899	0.834	0.870
Transmitter F	–	–	F1	8 Aug. 1989	4.5	(5)	0.413	0.244	0.104

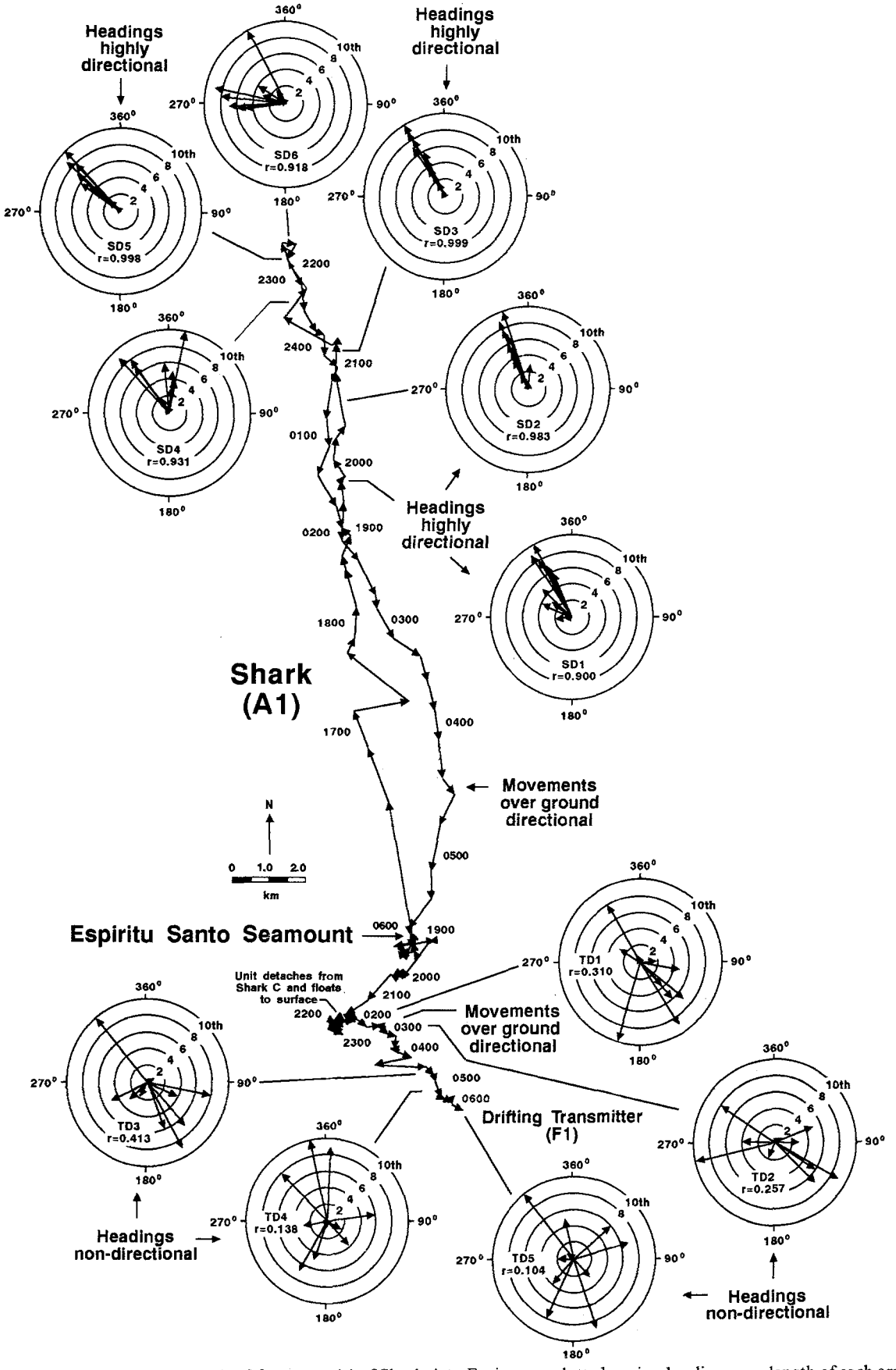

Fig. 4. *Sphyrna lewini.* Homing Movement A1 of Shark A to Espiritu Santo Seamount (arrow) and track (F1) of Transmitter F drifting away from seamount at sea surface after tag had become detached from Shark C; each track is comprised of vectors (arrows) drawn between successive positions of the shark determined at 15 min intervals; values by the vectors indicate time of day (hrs); shark swimming directions (SD) and transmitter drift directions (TD) are plotted as circular diagrams; length of each arrow in these diagrams indicates serial order of measurement, whereby shortest arrow designates direction recorded first and longest arrow direction recorded tenth and last. Although movements over ground of both shark and transmitter were oriented, only headings from the shark were highly directional

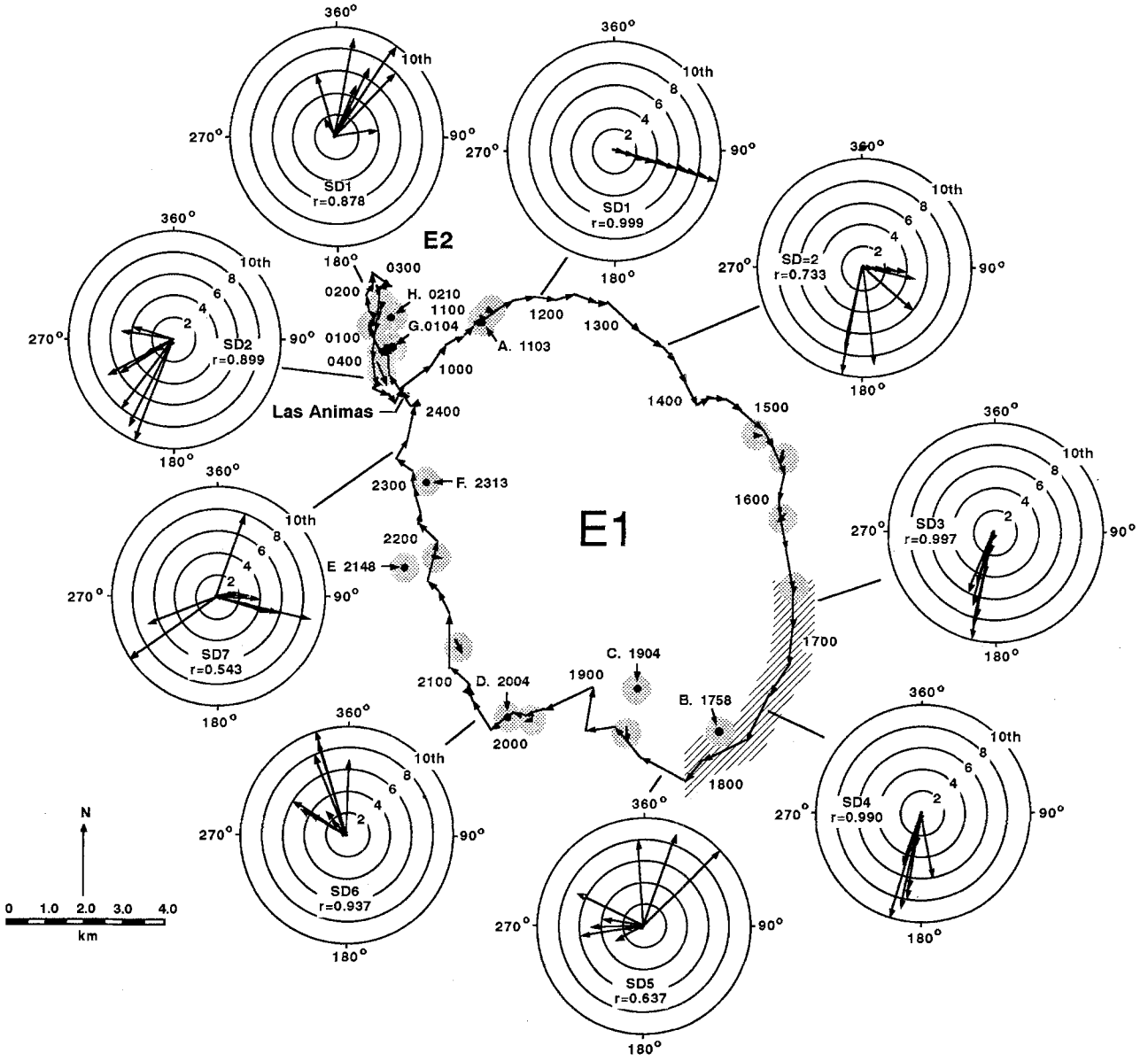

Fig. 5. *Sphyrna lewini.* Two homing movements (E1 and E2) of Shark E to Las Animas Island. Movement of surface water is indicated by length and direction of arrows inside stippled areas drawn between successive positions of drifter released near shark and allowed to float for same 15-min interval over which the shark's point-to-point movements were determined. Depth profiles of irradiance, temperature, and flow direction were made at locations (●) identified by letter and time of day (hrs). Hatching indicates area where 100 consecutive swimming directions of Shark E were recorded. Further details as in legend to Fig. 4

often only a fourth of the distance traveled by the shark during the same time period. This contrast was evident at 15.00, 16.00 and 22.00 hrs (see arrows inside stippled areas in Fig. 5). Furthermore, the water mass movements at 21.00 and 22.00 hrs were in a direction counter to those of the closest movements by the shark. At other times, the direction of the current was even perpendicular to the direction of the shark's movement over ground (11.00, 15.00, and 22.00 hrs: Fig. 5).

Although the movement over ground of a hammerhead stationary within a water mass would be oriented if flow were unidirectional, the heading of the shark would change unless maintained by forward momentum or attention to an external reference. This distinction is apparent from a comparison of the point-to-point movements and headings of Shark A with the directions recorded from the transmitter which drifted at the sea surface after it had become detached from Shark C following Homing Movement C6 (F1 in Fig. 4). The coefficients of concentration for the movements of Shark A along its outward and return paths of Homing Movement A1 were 0.782 and 0.905, respectively, and the coefficients for headings recorded during the track ranged from 0.900 to 0.999 (SD1–SD6 in Fig. 4), with a mean of 0.955. The movements of the transmitter over ground after ebb tide at 02.00 hrs were directional ($r=0.614$) yet smaller than those of Shark A. In contrast, the directions recorded from the drifting transmitter (TD) varied greatly, with coefficients ranging from only 0.104 to 0.413 (TD1–TD5 in Fig. 4), with a mean of 0.244.

One source of swimming directionality could be the shark's inertial movement forward. This could bias the

distributions of headings toward directionality, particularly if the intervals between successive measurements were short. In order to evaluate this bias, the intervals between successive swimming-direction measurements were extended to establish the period over which the shark maintained directionality to its swimming movements. Used in this analysis were samples of 100 consecutive directional measurements recorded from the drifting transmitter and Shark E (hatched section of E1 track in Fig. 5). During this period, the direction of the shark's movements over ground gradually changed in direction from south to southwest. The number of measurements (n) skipped between the next measurement was incremented by 1 for the first six sets of ten measurements and by 2 for the final two sets (Table 3). Thus, in set SD_{n+1}, every second directional measurement was used, in SD_{n+2} every third, and so forth until every tenth measurement was used in the calculation for SD_{n+9}. The mean direction for the sets rotated from 191.3° for set SD_n to 222.3° for set SD_{n+9}, indicating a change in the heading of the swimming hammerhead to a more westerly direction. Coefficients exceeding 0.900 were recorded for the headings of the shark throughout the first five periods, the last interval being 31 min 44 s long (see Table 3). It is doubtful if directionality could be maintained over this time period solely by swimming inertia.

Relationship to subsurface irradiance and temperature

Possibly the sharks could rely upon vision to swim along a ridge or valley in the sea floor or move toward the blurry image of the sun or moon. Actually, this was unlikely, because the sharks swam up and down in mid-water away from both the sea surface and bottom. For example, Shark E moved between 25 m and 300 m during the day and between 125 and 400 m at night (Fig. 6). During her first homing movement, Shark E moved in water over 732 m (= 400 fathoms) deep, over 300 m deeper than the lower dive limit of the shark. Only at 18.00 hrs did the hammerhead approach the surface, where it might see the image of the sun. Furthermore, extremely low levels of photopic and scotopic irradiance were recorded at the depths at which the shark swam (see 23.00 to 02.00 hrs, Fig. 6A, B). The depth trace of the shark extended below the photopic irradiance isolumin of 0.0001 $\mu W\ cm^{-2}\ s^{-1}$ and scotopic isolumin of 0.001 $\mu W\ cm^{-2}\ s^{-1}$. At the same time, the headings recorded from Shark E were highly directional, with a coefficient of concentration of 0.937 (SD 6 in Fig. 5).

The hammerheads did not favor those depths with steep vertical temperature gradients which would be accompanied by changing current speeds and directions, thus providing information potentially useful in guiding the sharks' movements. Two layers of water with different thermal gradients were evident in the temperature record (Fig. 6C). A large change in temperature with increasing depth was apparent near the surface from the closely spaced isotherms: a more gradual change at greater depth was evident from less closely spaced isotherms. The boundary to these two water masses was at 50 m. At this depth, the flow direction rotated from north to west along much of Shark E's path (see arrows on Hydrographic Casts B–E in Fig. 6D), indicating that the movement of the two layers was independent (locations of these casts are shown by arrowed data points in stippled areas in Fig. 5). Shark E's diving excursions were usually below the boundary to the two layers, where flow direction changed and could provide potential information relative to directional origins of either water mass. Yet at these times, the shark swam in a highly directional manner, with coefficients of concentration for its telemetered headings ranging from 0.637 to 0.937.

Homing movements along fixed geographic paths

Fourteen homing movements to and from Espiritu Santo Seamount by three hammerhead sharks were tracked (Fig. 7). The tracks are composed of lines drawn between positions determined at 15 min intervals, with arrows indicating the direction of movement. Two of these vectors were considered to occur over the same geographic path if the 75th percentile error band to either side of one vector overlapped the error band of the other vector. The error bands at successive distances from the seamount are

Table 3. *Sphyrna lewini.* Descriptive statistics for sets of ten swimming directions (SD) taken over time intervals of increasing length from 100 consecutive measurements recorded from Shark E during Track E1 (hatched section of track in Fig. 5). Interval was increased by using every nth measurement. In SD_{n+1} every second swimming direction was used, in SD_{n+2} every third, and so forth until in SD_{n+9} every tenth heading was used in calculation. (N): no. of measurements. n: no. of measurements skipped between next measurement in set

Set No.	Time of day (hrs.min/s):		Time interval (h/min/s)	Swimming direction			
	initial	final		Measurement schedule	(N)	Mean (deg)	Coef. conc. (r)
1	16.24/07	16.25/32	1/25	n	(10)	191.3	0.999
2	16.24/14	16.35/32	11/18	$n+1$	(10)	201.8	0.948
3	16.24/29	16.43/14	18/35	$n+2$	(10)	195.7	0.995
4	16.24/42	16.50/50	26/08	$n+3$	(10)	206.8	0.920
5	16.24/49	16.56/33	31/44	$n+4$	(10)	202.6	0.959
6	12.24/58	16.58/35	33/37	$n+5$	(10)	218.1	0.736
7	16.25/18	17.29/13	1/03/55	$n+7$	(10)	208.3	0.939
8	16.25/32	18.00/52	1/35/20	$n+9$	(10)	222.3	0.838

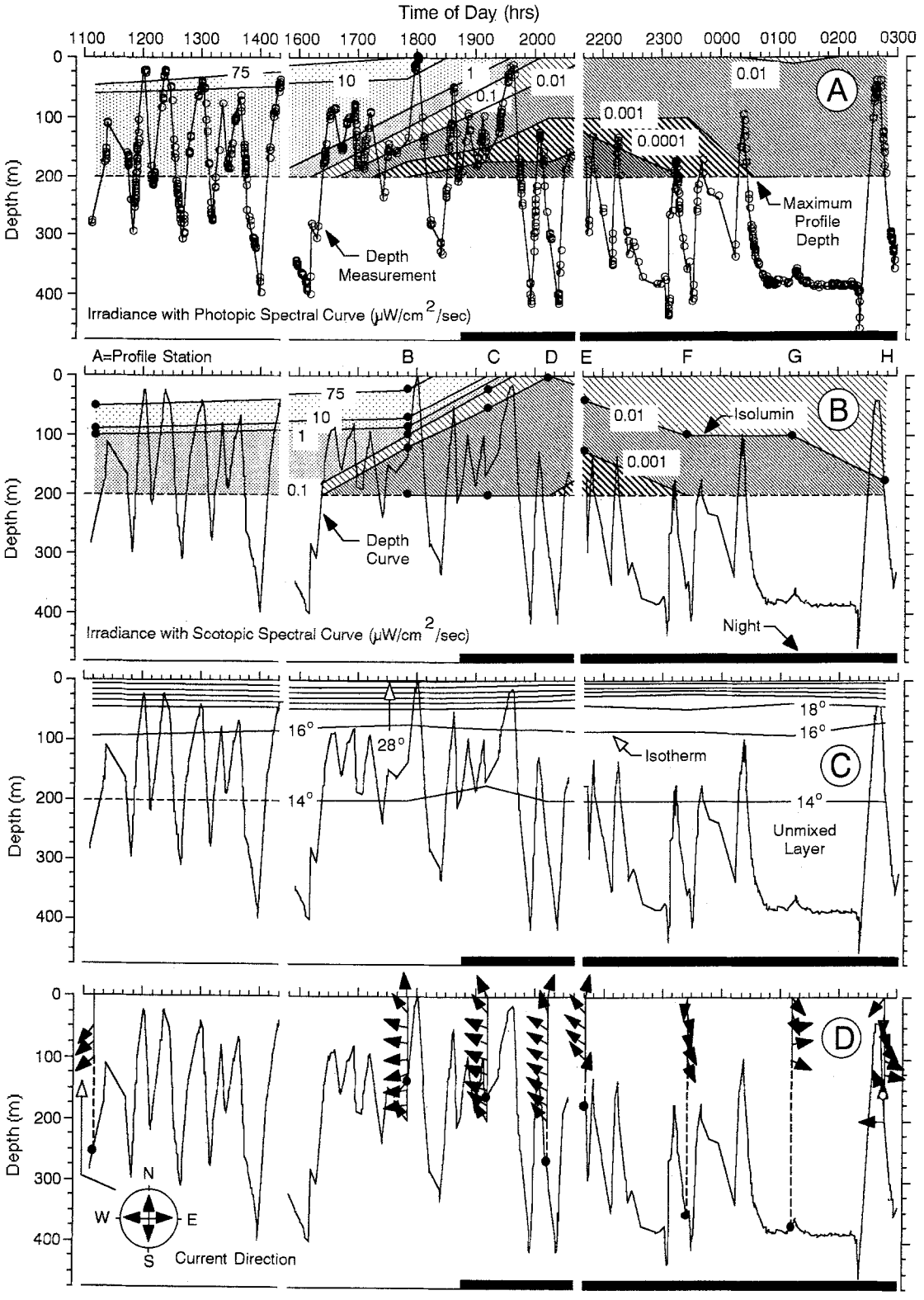

Fig. 6. *Sphyrna lewini.* (A) Depths of Shark E superimposed upon isolumes indicating level of photopic irradiance in water column near shark; measurements are indicated by open circles connected by continuous lines. (B) Depths of Shark E in relation to distribution of scotopic irradiance. (C) Depths of Shark E relative to vertical distribution of temperature in water column; unlike for salmon (Westerberg 1982b, 1984), oscillatory swimming movements of Shark E rarely crossed boundary (at 50 m) between two water masses, indicated by change in spacing between isotherms. (D) Depths of Shark E in relation to directions of water flow in the water column at points along path of Shark E; vertical lines indicate time of hydrocasts, with continuous lines denoting those depths at which measurements were taken and dashed lines greater depths; a circle on a line indicates that the hydrocast depth was equivalent to the depth of Shark E at that time; black arrows denote flow directions relative to compass rose at lower left. Irradiances, temperatures, and flow directions were measured at 25 m depth intervals to depth of 200 m at points along the shark's path. Lettering between Graphs (A) and (B) indicates times at which hydrocasts were made; locations of stations are plotted in Fig. 3

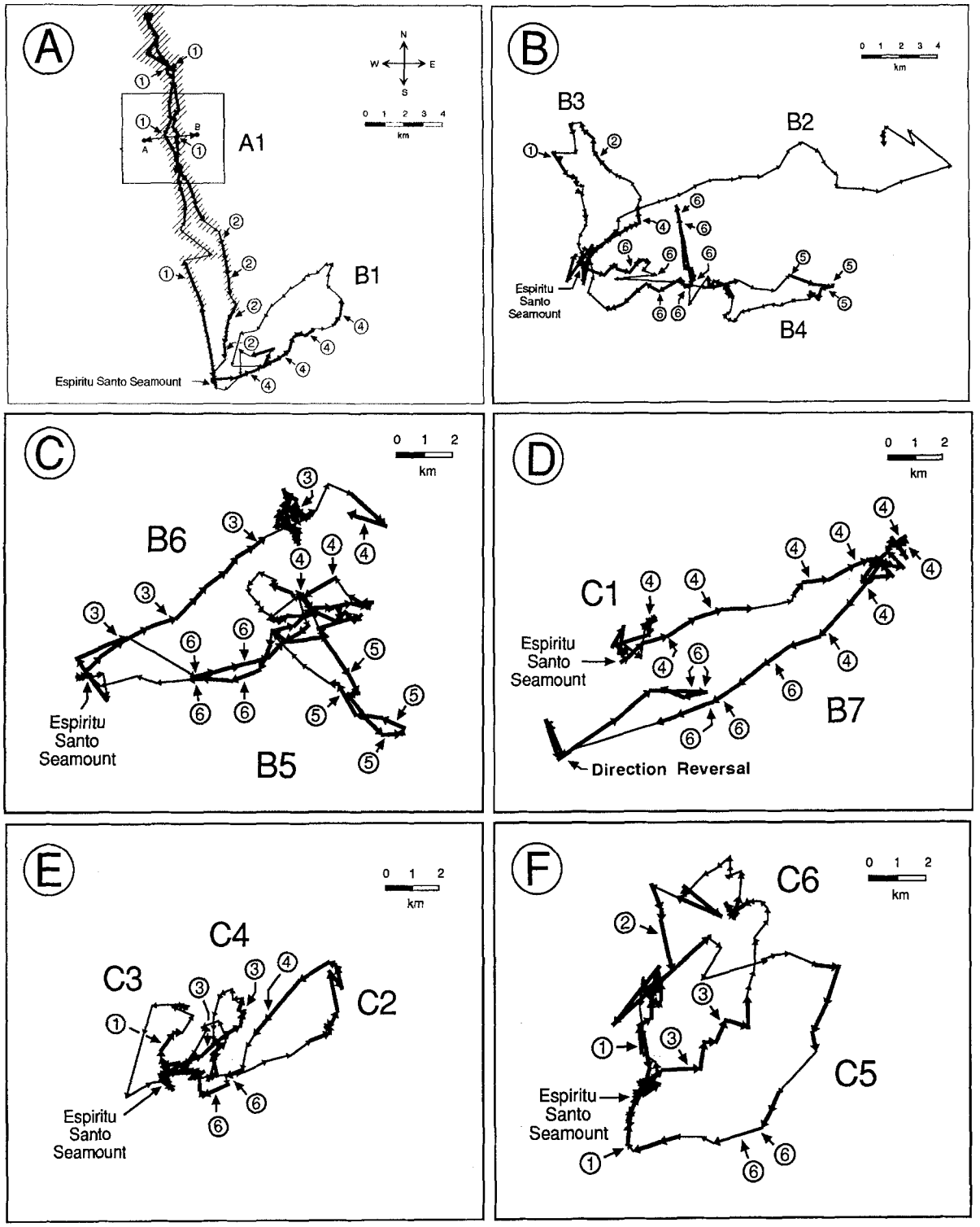

Fig. 7. *Sphyrna lewini.* Homing Movements A1, B1-7, and C1-6. Each movement is composed of vectors between successive positions determined at 15 min intervals with an arrowhead indicating direction of movement. Heavier portions of lines indicate that one or more movements occurred over same geographic path, based upon overlap of 75th percentile spatial error bands to vectors from both tracks. Extent of positional error at different distances from the seamount is illustrated by hatched areas on outward and return movements of Track A1. Measurements of magnetic field intensity were made at 25 m depth intervals at Points A and B (see boxed-in area around Track A1 in Fig. 7A) Homing movements occurred primarily over six paths, designated by circled numbers 1–6, which will be later shown in this paper to coincide with the locations of ridges and valleys leading away from the seamount in the topography of geomagnetic intensity

indicated for A 1 (hatched areas in Fig. 7 A). Overlapping vectors are indicated by thick lines, non-overlapping vectors by thin lines. Those parts of homing movements occurring along a common geographic path are apparent from the thickness of the vectors.

The hammerheads swam repeatedly along the same geographical paths. This was evident from those sections of each track with heavily marked vectors, indicating movement of one hammerhead over the same path as another. Six paths were used repeatedly by Hammerheads A–C during their homing movements to and from Seamount Espiritu Santo. The first path led along a north-south axis away from the seamount (Labelled 1 in Fig. 7 A–B, E–F). Shark A moved out and back along this path when farthest from the seamount (Fig. 7 A). Sharks B and C returned to the seamount several times over part of the outward path previously taken by Shark A. Note the heavily marked vectors during the return of B 3 to the seamount (Fig. 7 B) and during both the outward and return movements during Tracks C 5 and C 6 near the seamount (Fig. 7 F). A second path existed slightly eastward of the first. The outward and return movements of Hammerhead A diverged near the seamount, where it swam along Path 2 when returning (Fig. 7 A). Sharks B and C swam along this path during Tracks B 3 and C 6, respectively (Fig. 7 B, F). A third path was in a northeastern direction away from the seamount and was taken once by Hammerhead B (Path 3, Fig. 7 C) and twice by Shark C (Fig. 7 E–F). A fourth path, slightly to the east of the third, was taken by Shark B four times (Path 4, Fig. 7 A–D), and by Shark C a single time (Fig. 7 E). A fifth path existed along a southeast axis distant from the seamount, and was followed by Shark B during Movements B 4 and B 5 (see Path 5, Fig. 7 B, C). Finally, the sixth path extended east of the seamount and was evident from the coincidence of movements during Tracks B 4, B 5, and B 7 of Shark B and during Tracks C 4 and C 5 of Shark C (Fig. 7 C–F).

Relationship to bathymetry

The seamount is located on the southern end of a ridge with it's long axis in a north-south direction (Fig. 8 A). The ridge slopes to a depth of 1000 m at its northern end, 500 m to the east, 700 m to the south, and 800 m to the west. A deep canyon separates the ridge from another ridge to the east. South of the shallow areas is a deep valley which extends in a southeast-northwest direction, widening farther north.

There was no consistent relationship between the paths of the homing sharks and ridges and valleys in bottom topography leading away from the seamount. Although those parts of the tracks of all three sharks along Paths 1 and 2 (Fig. 7) were along the ridge along a north-south axis (Fig. 8 A), the sections of track associated with Paths 3 to 6 passed over the eastern slope of the seamount, across the flat ocean basin to the east, and then over the western slope of the ridge to the east of the seamount. The motivation for the sharks to visit the eastern seamount may have been the local abundance of prey. Indeed, parts of Track B 6 and B 7 near the eastern ridge were comprised of clusters of small movements in widely varying directions, indicating that the sharks may have been feeding. These random movements contrasted greatly with the tracks of the sharks to and from this point, composed of large movements in one direction. The clumped movements resembled those of the drifting transmitter at ebb tide, and may have been due to drift. In contrast, the highly oriented movements between the two ridges could not be carried out without an environmental reference.

There was little clumping of shark positions at peaks of the positive and negative excursions of the depth trace on the bathymetric record from underwater ridges and valleys (Fig. 9). Only 41% (65 of 158) of the shark positions were associated with $\geq 20°$ changes in slope of the trace of bottom depth using the median as a criterion of positional accuracy (Table 4). Using the least rigid standard of accuracy, the range, only 61% (96 of 158) of the shark positions were associated with a change in slope. Similarly, 43% (68 of 158) and 67% (105 of 158) of the points from the track simulations were associated with the slope discontinuities based upon the above-mentioned two levels of positional accuracy. The percentages of shark positions associated with slope changes did not differ from the percentages of simulation points in a statistically significant manner (Table 4). Indeed, the records from the simulations (Fig. 9 E, F) closely resembled the records from the shark tracks (Fig. 9 C, D) in the absence of clumping of points at peaks and valleys.

Relationship to geomagnetic field

The seamount is situated on the edge of a geomagnetic plateau exhibiting little magnetic relief but having a steep slope of rapidly decreasing magnetic intensities to the west (Fig. 8 B). The edge between the slope and plateau is roughly along a north-south axis. Extending away from the seamount on the plateau are small valleys and ridges in the magnetic relief (stippled areas and circled numbers 1–6 in Fig. 8 B). If detectable by the sharks, these features in the topographic relief of geomagnetic intensities could provide reference paths over which to move back and forth to the seamount.

The geomagnetic relief in the area of the seamount was more evident on the curve of intensities recorded as a magnetometer was towed in concentric circles around the seamount (Fig. 10). Continuous records (Symbols A–D in Fig. 10) of geomagnetic intensity were obtained by towing the magnetometer along the four circular paths nearest to the seamount (Fig. 2 A). The geomagnetic plateau was apparent on the right and left side of each record as undulations in the intensity curve, with less than a 50 nT rise or fall between successive maxima and minima (Fig. 10 A). The plateau extended from the record's left edge, a point on the circle directly east of the seamount, to a point roughly south of the seamount (Fig. 2 A). The westward slope south of the seamount was apparent as many closely-spaced and steep traces sloping downward to the right (Fig. 10 A), indicating a rapid de-

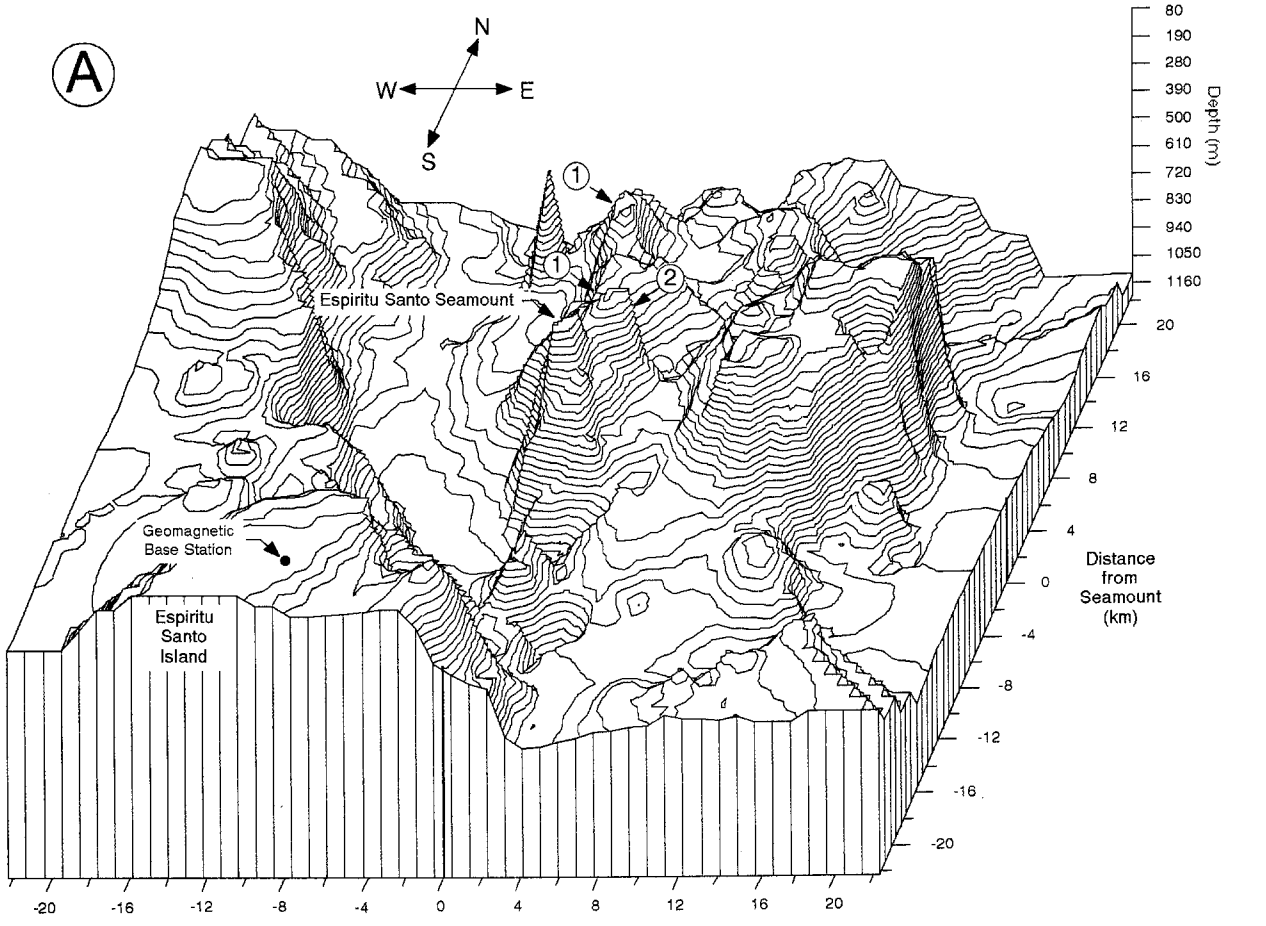
A
N
W
E
S
Espiritu Santo Seamount
Geomagnetic Base Station
Espiritu Santo Island
Depth (m)
80
190
280
390
500
610
720
830
940
1050
1160
Distance from Seamount (km)
20
16
12
8
4
0
-4
-8
-12
-16
-20

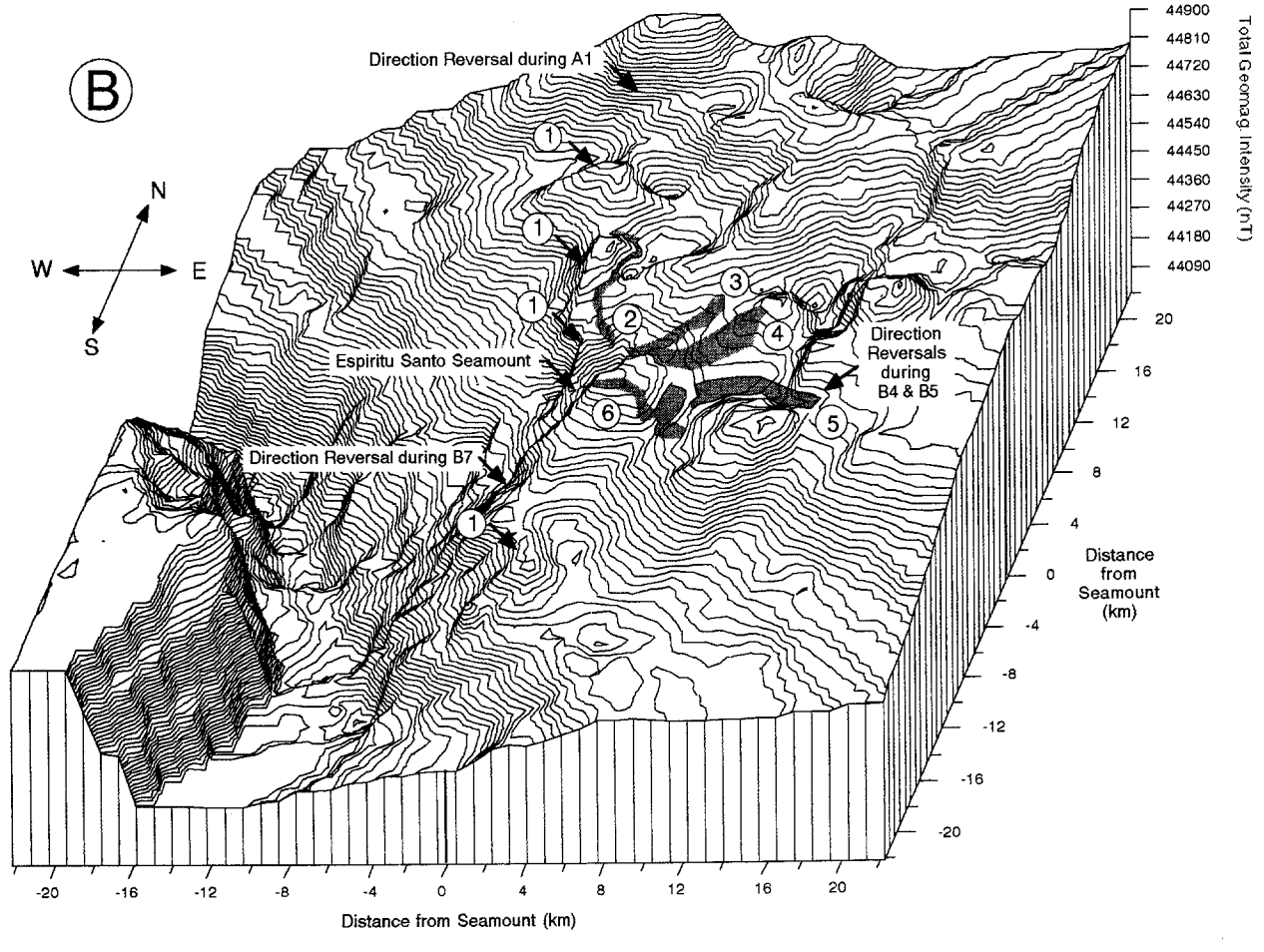
B
Direction Reversal during A1
N
W
E
S
Espiritu Santo Seamount
Direction Reversals during B4 & B5
Direction Reversal during B7
Total Geomag. Intensity (nT)
44900
44810
44720
44630
44540
44450
44360
44270
44180
44090
Distance from Seamount (km)
-20
-16
-12
-8
-4
0
4
8
12
16
20

Table 4. *Sphyrna lewini.* Number (and % of total) of points on bathymetric record associated with positive and negative excursions of depth trace indicating that sonar passed over submarine ridges and valleys based upon the median, 75th percentile, and range of positional accuracy. Comparison is made between points from sharks' tracks and those from simulations. Note that proportions of those points with and without positional errors overlapping 20° discontinuities in trace slope for the two types of points did not differ in statistically significant manner for any of three criteria of accuracy. Statistical significance: significance of difference between proportion of points with overlap to total of points for track versus simulation using chi-square test. NS: $p<0.05$

Criterion of accuracy	Track *N* (% total)	Simulation *N* (% total)	Statistical significance
Median			
overlap	65 (41%)	68 (43%)	0.5325 (NS)
non-overlap	93 (59%)	90 (57%)	
total	158	158	
75th percentile			
overlap	69 (44%)	78 (49%)	0.3101 (NS)
non-overlap	89 (56%)	80 (51%)	
total	158	158	
Range			
overlap	96 (61%)	105 (67%)	0.2927 (NS)
non-overlap	62 (39%)	53 (33%)	
total	158	158	

crease in magnetic intensity recorded as the magnetometer was towed in a clockwise path around the seamount away from the geomagnetic plateau and over the slope. These lines ended in an apparent valley almost directly west of the seamount (W, Fig. 2A) followed by many closely-spaced and steep traces sloping upward to the right (Fig. 10A), indicating an abrupt increase in the magnetic intensity recorded as the magnetometer was towed clockwise back over the geomagnetic slope to the west of the seamount and over the plateau. The plateau began almost directly north of the seamount ("N", Fig. 2A), and was evident from the appearance again of undulations in the trace of geomagnetic intensities (Fig. 10A).

Few shark positions occurred on the steep slopes of the trace that indicated total geomagnetic intensity on the records. Because the magnetometer was towed at a constant speed, the slope of the trace was an indicator of the geomagnetic gradient, the intensity change per unit distance. A steep slope on the trace thus indicated the presence of a strong magnetic gradient across the sea floor.

Fig. 8. (A) Bathymetry at Espiritu Santo Seamount in Gulf of California with 50 m depth contours; note seamount is located at southern edge of a submarine ridge extending along north-south axis. (B) Magnetic total field intensities at seamount with 10 nT contour intervals; note western geomagnetic slope and eastern plateau with small hills, ridges, depressions, and valleys in geomagnetic topography from seafloor magnetization; ridges and valleys in geomagnetic topography are indicated by stippling. Numbers on both maps correspond to paths taken repeatedly by homing sharks, *Sphyrna lewini*

Four shark positions occurred on the steep magnetic slope west of the seamount (Fig. 10C). These were associated with a reversal in the shark's swimming direction (Track B7 in Fig. 7D). On the other hand, most of the sharks' locations on the records were clustered at maxima and minima in the intensity trace that were preceded and followed by steep slopes. For example, see the five points indicating sharks at the maximum at Magnetometer Position 8 in Fig. 10C and three at the minimum near Magnetometer Position 48 in Fig. 10B. However, points also occurred at large angular changes in steep continuous slopes. Note, for example, the cluster of six points on the small discontinuity in the slope of the maximum in the trace between Magnetometer Positions 6 and 7 on Record D (Fig. 10). Four more points occured at a similar break in the intensity trace from the same maximum at Magnetometer Position 23 on Record C. Furthermore, flat maxima and minima in the trace often had points at their edges. For example, four points occurred at the edge of the flat maximum at Magnetometer Position 7 on Record D. Points indicating sharks also coincided with the edges of the flat intensity minimum at Magnetometer Positions 91 and 92 on Record A. Almost all of these points were associated with a break in the slope of the magnetic intensity trace, suggesting that the shark oriented to a change in geomagnetic intensity gradient rather than simply to a maximum or minimum.

The same slope breaks, maxima, and minima could be located on all four records, each successively farther from the seamount, because the magnetometer, towed around the seamount in concentric circles, produced records which were cross-sections of the edge to the geomagnetic plateau or small ridges and valleys leading away from the seamount on the plateau (stippled areas numbered 1–6 in Fig. 8B). A shark could move back and forth to the seamount using these features by avoiding locations with strong magnetic gradients or seeking areas with sharp changes in the gradient.

The points from homing movements occurred on maxima and minima from the same ridges and valleys on successive concentric geomagnetic records at increasing distances from the seamount. The most prominent feature in the geomagnetic relief of the survey area was the edge between the western slope and eastern plateau (Path 1 Fig. 8B). This boundary extended across the entire survey area in a north-south direction and separated the survey area into halves. The seamount was located on the edge between the plateau and slope near the center of the survey area. The three sharks tracked during this study as well as a fourth tracked during an earlier study moved along this boundary. North of the seamount the boundary between the geomagnetic slope and plateau is apparent on Records A–D as the first maximum to the right of many closely-spaced traces, and south of the seamount to the left of many closely-spaced traces (see Path 1, Fig. 10). The outward path of Shark A was along this path (Fig. 10A–D). Shark B returned to the seamount along this ridge (Fig. 10B–D), as did Shark C twice (Fig. 10D). In an earlier study, Shark D (see Track No. 9 in Fig. 6 of Klimley and Nelson 1984) moved along the edge of the slope south of the seamount (Fig. 10B, C).

Hammerheads also moved along geomagnetic valleys (Paths 2–3, and 5 in stippled areas in Fig. 8 B). Although the outward and return movements of Hammerhead A along Track A 1 followed the same path at greater distances from the seamount, at closer distances Shark A's outward and return movements were separated (Paths 1 and 2 in Fig. 7 A). Here, the shark returned along a geomagnetic valley. This is apparent from the coincidence of the filled circles indicating the shark's positions with steep and narrow minima at Magnetometer Positions 6, 20, 47, and 86 on the four concentric records nearest the seamount (Path 2 in Fig. 10 A–D). Return movements of Sharks B and C were along the same geomagnetic valley, as evidenced by the open circles and filled squares indicating these sharks' positions at the bases of the same minima. Sharks B and C also swam back and forth along another geomagnetic valley leading from the seamount in a northeasterly direction (Path 3 in Fig. 10 A, B).

The movements of Sharks B and C occurred along two geomagnetic ridges, one in a northeastern direction and the other an eastern direction (Paths 4 and 6 along stippled areas in Fig. 8 B). Of particular interest is the movement of Hammerhead B during Track B 4. On the magnetometer record, the shark's movement along the ridge is apparent from the open circles indicating shark positions present at maxima (Path 6 on Fig. 10 B and C). However, on Record A the points are on two adjacent maxima separated by a minimum where the ridge and diverged, permitting the sharks to move along the forked ridges separated by a valley (Path 5, Fig. 10 A). The forked ridges and separating valley are both apparent on the 3-D map of the geomagnetic topography surrounding the seamount (Paths 5 and 6 along stippled areas in Fig. 8 B). The shark made a perpendicular turn to swim along the north-south oriented ridge. This directional change is evident on Track B 4 of Fig. 7 B as antiparallel movements north and south, perpendicular to east-west oriented sections of the track before and after the movement.

Comparison of the direction reversals of homing movements to features in the geomagnetic field yields some insight into the travel strategy of the sharks. For instance, Shark A swam along the edge of the geomagnetic plateau until it reached the base of a steep geomagnetic hill, when it reversed direction (Track A 1 in Fig. 7 A and Path 1 in stippled area on Fig. 8 B). Furthermore, Shark B swam along Path 5, following a geomagnetic valley during Homing Movements B 4 and B 5 until the valley was blocked by a steep slope, at which point Shark B reversed direction. Not only did the sharks change direction upon encountering steep gradients, with magnetic intensity increasing in the direction of movement, but the same response was shown when encountering a strong gradient with intensity decreasing in the shark's swimming direction. For instance, Shark B reversed direction during Track B 7 immediately upon swimming over the steep geomagnetic slope west of the seamount. The initial

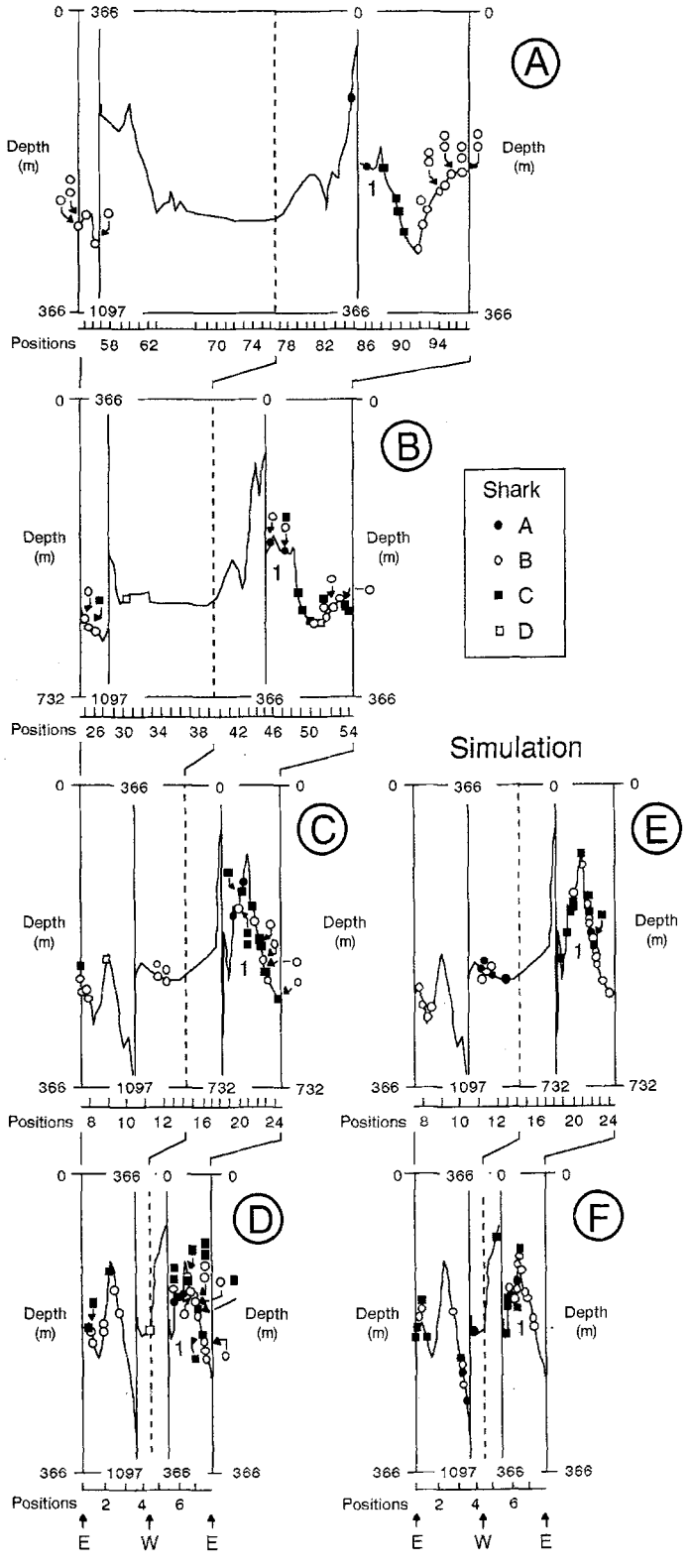

Fig. 9. *Sphyrna lewini.* (A)–(D) Continuous sonar records of bottom depth for four concentric survey circles nearest seamount; changes in depth scales are indicated by continuous vertical lines, upper and lower depth limits are given on upper and lower abscissas; positions on record where Sharks A–D crossed path of the sonar are indicated by relevant symbols (see "key"); although some shark positions were along a submarine ridge designated Path 1 (Fig. 8 A), many shark positions were not confined to positive and negative excursions in the traces of bottom depths indicating the presence of submarine ridges and valleys. (E), (F) Positions on sonar record for simulations for Tracks A–D, denoted with relevant symbols; distribution of these points differed little from distribution of points from actual track

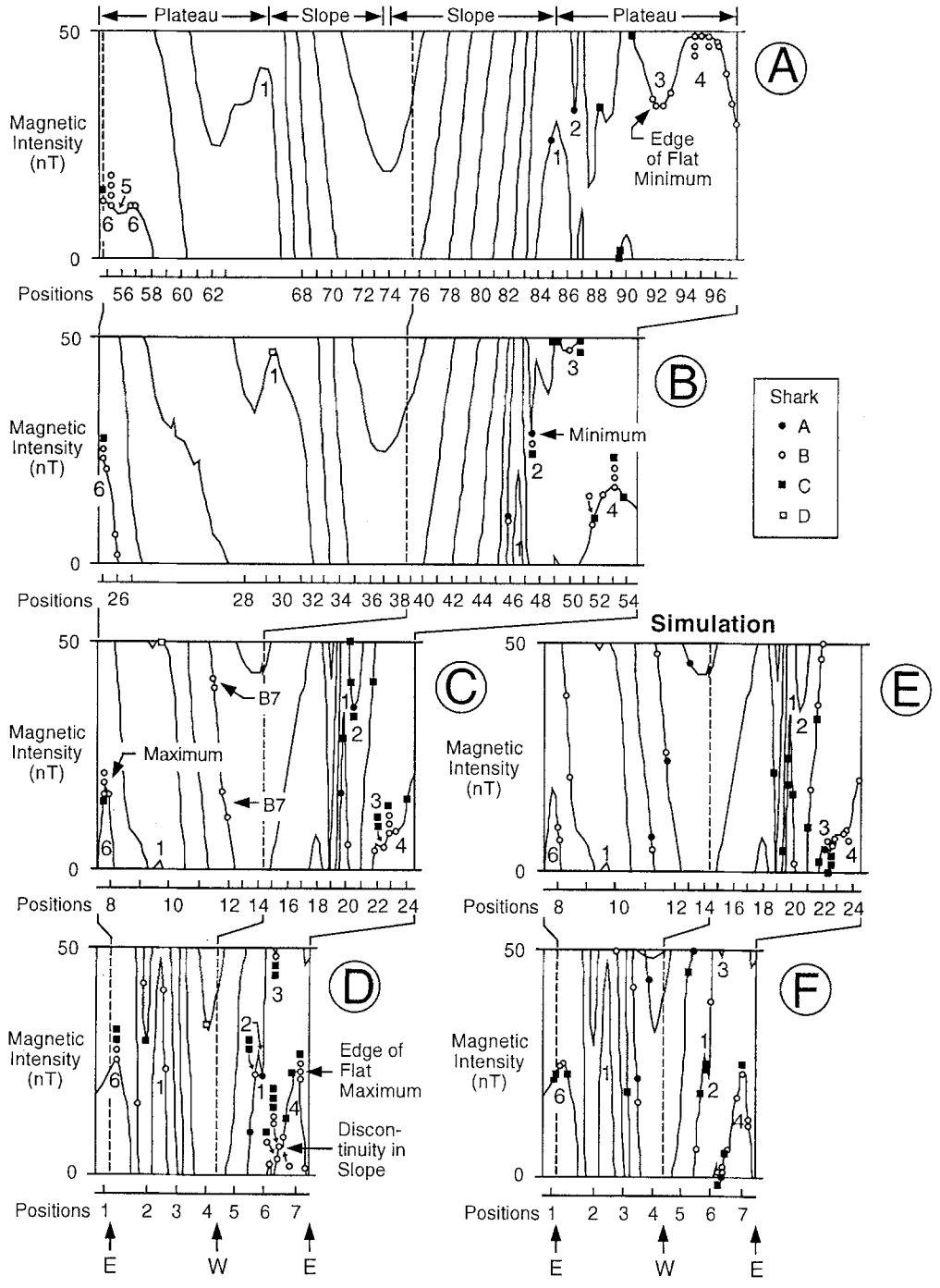

Fig. 10. *Sphyrna lewini.* (A)–(D) Continuous magnetometer records of total geomagnetic field intensity for four concentric survey circles nearest to seamount; positions on record where Sharks A–D crossed path of the magnetometer are indicated by relevant symbols (see "key"); 1–6 identify maxima and minima in the intensity traces on each record from Ridges and Valleys 1–6 in geomagnetic topography leading from the seamount (shown by stippled areas on contour map of magnetic relief: Fig. 8B) and also Paths 1–6 along which Sharks A–C repeatedly swam (heavier lines on tracks which indicate spatial overlap in Fig. 7); note that points denoting shark positions were clustered at maxima and minima on the records. (E), (F) Points on records from simulations for tracks of Sharks A–D, distinguished by different symbols; note that these points were displaced away from maxima and minima on the records; e.g. compare track points for Maximum No. 6 in (D) with simulated points for same peak in (F)

response of the shark upon encountering such a gradient was to reverse direction and swim in a direction perpendicular to the contour lines.

If sharks swim along ridges and valleys in the topography of geomagnetic field intensities, the shark positions should be clustered at either maxima and minima in the traces on the magnetometer records. However, two changing geomagnetic gradients could occur if the ridge were flattened at the top or if the bottom of the valley were wide. Shark positions were also clustered at these locations on the record (see maximum for Ridge 4 in Fig. 10D and minimum for Valley 3 in Fig. 10A). In fact,

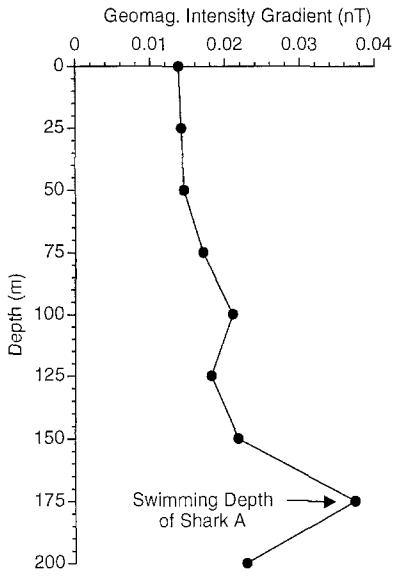

Fig. 11. Magnitude of magnetic intensity gradient as a function of depth. Gradient consists of difference between magnetic intensities measured to a depth of 200 m at 25 m depth increments at Stations A and B (boxed-in area on Fig. 7A) divided by separation distance. *Sphyrna lewini* A swam highly directionally at a depth of 175 m (SD1 in Fig. 4)

Table 5. *Sphyrna lewini.* Number (and % of total) of points on magnetometer record associated with maxima and minima in the trace indicating that magnetometer was towed over geomagnetic ridges and valleys based upon the median, 75th percentile, and range of positional accuracy. Comparison is made between points from sharks' tracks and those from simulations. Much greater proportion of points from sharks' tracks were associated with 20° slope discontinuities than for simulation points. This difference was highly statistically significant at all three levels of positional accuracy. Statistical significance: significance of difference between proportion of points with overlap to total of points for track versus simulation using chi-square test

Criterion of accuracy	Track N (% total)	Simulation N (% total)	Statistical significance
Median			
overlap	102 (76%)	82 (52%)	<0.0001
non-overlap	38 (24%)	76 (48%)	
total	158	158	
75th percentile			
overlap	123 (78%)	89 (56%)	<0.0001
non-overlap	35 (22%)	69 (44%)	
total	158	158	
Range			
overlap	143 (91%)	124 (78%)	<0.0001
non-overlap	15 (9%)	34 (22%)	
total	158	158	

shark positions were also common where the rising or falling intensity trace flattened temporarily before continuing with the same slope (see ledges between Magnetometer Positions 6 and 7 in Fig. 10D and 21 and 22 in Fig. 10C). For these reasons, an objective yet general definition of gradient boundary was used for the statistical comparisons: a $\geq 20°$ angular change in the slope of the intensity trace on the magnetometer record for association of the shark's position with a maximum or minimum in the magnetic intensity record (overlap criterion in Fig. 2).

The association between homing movements and geomagnetic gradient boundaries was apparent when the positions of the track-intersection points were compared to points on the record from the simulated track vectors. The shark positions were clustered at maxima and minima in intensity traces on the four magnetometer records, indicating ridges and valleys leading away from the seamount on the geomagnetic plateau, and were absent from the continuously ascending or descending traces, indicating that the magnetometer passed over the geomagnetic slope west of the seamount (Fig. 10A–D). Seventy-six percent of the shark positions (120 of 158) overlapped a slope change of $\geq 20°$ using the median accuracy as a criterion of overlap (Table 5). Ninety-one percent of the positions (143 of 158) overlapped that slope change using the range of accuracy as an overlap criterion. On the other hand, points from the track simulations were not generally clustered at maxima and minima (Fig. 10E, F). Fifty-two percent of the simulation points (82 of 158) overlapped a slope discontinuity within the median positional error and 78% of the points (124 of 158) based upon the range of error. A significantly greater proportion of track points overlapped geomagnetic features than did the simulation points (chi-square, test of independence, $N=316$, $p<0.001$).

The magnitude of the geomagnetic gradient was determined at the depth at which Hammerhead A was swimming highly directionally. Hammerhead A was tracked along the edge of the geomagnetic plateau (track in boxed area on Fig. 7A, for field see Figs. 8B, 10). The intensity difference was determined between Locations A and B on either side of Track A1 (Fig. 7A). Shark A passed between Locations A and B at 19.38 hrs. The headings were highly directional, with a coefficient of concentration of 0.900 (SD1, Fig. 4). At this time, the hammerhead swam at a depth of 175 m on the downward trajectory of an oscillatory vertical swimming path (own unpublished data).

At the surface the gradient was 0.0138 nT/m, at 200 m 0.024 nT/m (Fig. 11). Of particular interest was the magnitude of the gradient at the 175 m depth at which the shark swam. Here the strength of the gradient was 0.0374 nT/m, the maximum recorded in the water column and greater than that measured 25 m deeper at 200 m. This departure from a linear increase in magnetic gradient with increasing depth suggested the presence of another magnetic source near the surface, which contributed on the horizontal plane to the magnetic field surrounding the seamount, in addition to the sea floor magnetization immediately below the two points, which contributed to the field on the vertical plane. A magnetic deposit located near the peak of the seamount would increase the total geomagnetic field intensity recorded at the depth of this magnetic source more than at points higher and lower in the water column.

Discussion

Highly directional swimming

High directionality is characteristic of the point-to-point movements of salmons (Westerberg 1982a, Quinn et al. 1989), scalloped hammerhead (Klimley and Nelson 1984), and blue sharks (Landesman 1984, Carey and Scharold 1990). A high degree of straightness to point-to-point movements, however, does not necessarily indicate directional swimming. Such movements could result if the fish were stationary in a water mass moving swiftly in a single direction. R. Brill et al. (personal communication) found that the straight-line movements of marlin are deflected with shifts in current direction, implying that the directionality to these movements over ground is partly due to drift in the ocean current. The point-to-point movements of the transmitter tracked at the sea surface during the present study on *Sphyrna lewini* were also highly directional, although the orientations of the drifting transmitter varied greatly. In contrast, highly directional swimming directions were telemetered from the hammerheads while they moved over ground in a highly directional manner. In addition, the point-to-point movements of Sharks A and E were frequently four times the distance of the movements of the transmitter which had become detached from Hammerhead C and of the drifter deployed near Shark E. The highly directional swimming of the hammerheads, sustained for long periods of time, suggested the use of some environmental property to guide hammerhead sharks to the seamount.

Subsurface irradiance and temperature

Vision may be of reduced importance to animal navigation in the marine environment because of its dependence upon irradiance, which is absorbed and scattered quickly in sea water. While birds at any height can fly directionally by moving toward a visual reference point such as the sun, moon, star pattern, or landmark, fishes can accomplish this only by swimming close to the surface through which the sun appears as a blurry, bright spot or close to the bottom where fishes can swim parallel to a ridge or valley. Orientation to the sun may occur at least in shallow water. Lemon sharks (*Negaprion brevirostris*) in a shallow lagoon changed swimming direction from east to west at sunset and from west to east at sunrise (Gruber et al. 1988). The movements toward shore of parrot fishes were less directional when their eyes were covered with opaque cups than with transparent cups and when the sun was blocked by clouds (Winn et al. 1964).

It is doubtful that hammerheads maintained directionality to their movements by keeping visual contact with the bottom or sea surface. Straight-line swimming could be the result of swimming along a ridge or valley on the bottom or toward the blurry image of the sun or moon. Yet the hammerhead sharks tracked during this study rarely approached either the sea floor or water surface, but swam up and down in the middle of the water column.

It is unlikely that even polarized light either from the sun or, less likely, the moon, could provide guidance to the scalloped hammerhead swimming at considerable depths. The polarization of irradiance underwater is greatest perpendicular to and least in the direction of the azimuth of the sun (McFarland 1991), thus providing a directional reference. Sensitivity to polarized irradiance has yet to be demonstrated for an elasmobranch, but has now been shown in three bony fishes [i.e., halfbeak (Waterman and Forward 1972), goldfish (Hawryshyn and McFarland 1987), and juvenile trout (Hawryshyn et al. 1990)]. Even if the perceptual capability existed, the amount of polarized irradiance reaching the shark would be reduced greatly by reflection from particles suspended in the water column.

Were the levels of irradiance at the considerable depths at which hammerhead sharks swam sufficiently high for perception? And if this were so, did the irradiance originate from a celestial body, or alternatively did it originate near the shark from bioluminescent organisms at the depth of the sharks? During nighttime, the levels of photopic and scotopic irradiance were very low, $<0{,}0001$ and <0.001 $\mu W\ cm^{-2}\ s^{-1}$ at depths of 150 to 200 m, the uppermost limit to the vertical diving excursions of Shark E (Fig. 6). These levels were below the threshold levels of 2.263 and 0.115 $\mu W\ cm^{-2}\ s^{-1}$ for 0.02 s flashes of monochromatic light of 451 and 533 nm, those wavelengths to which lemon sharks were most sensitive, after light- and dark-adaptation (O'Gower and Mathewson 1967). Lower thresholds for perception of white light were recorded for initially light-adapted lemon sharks after increasing periods of dark adaptation (Gruber 1967). The threshold sensitivity increased from 2.45 $\mu W\ cm^{-2}\ s^{-1}$ after 2 min to only 0.00024 $\mu W\ cm^{-2}\ s^{-1}$ after 60 min, with a temporal variation of 1 log-unit. The latter sensitivity exceeds by 1 log-unit the scotopic irradiance level measured at the upper limit of the diving excursions of Shark E (Fig. 6B). The white light, on which these thresholds were based, had its electromagnetic energy distributed equally over a broad range of wavelengths unlike the narrow bandwidths of irradiance matching the photopic and scotopic spectral sensitivity curves of the shark used to calibrate the transmitter's sensors. Although insufficient irradiance was available for photopic vision, sufficient irradiance may have been present in the blue end of the spectrum for limited scotopic vision at the upper parts of the diving excursions. At the lowest parts of the excursions, the irradiance originating from the surface probably diminished to a level below the shark's visual sensitivity.

Thermal variation is greater in the ocean than in the atmosphere because mixing is less rapid in the former environment. The water column is comprised of thick layers of water, each distinguished by a continuous and gradual change in temperature per unit of depth and separated from others by thin transition zones with greater rates of thermal change (Westerberg 1984). Each layer has a unique geographic origin and moves on a horizontal plane with a different speed and direction. These different layers originate from distinct water masses. These are apparent at the sea surface as areas of water

with little temperature change, separated from each other by fronts with abrupt thermal gradients.

Westerberg suggested (1984) that fishes could gain the information needed to maintain a directional course from the discontinuous thermal gradient throughout the water column. The fish must first move up and down throughout the entire water column to identify that layer of water originating from its home stream based upon the presence of a site-specific olfactant. The swimming excursions would then be reduced to cross only the boundary between the layer originating from the site to which the fish seeks to return and the adjacent layer. The direction to the layer's origin could be distinguished from the change in tactile stimulation across the fish's body from different water motions, a visually perceived difference in the direction of drifting particles, or a change in the voltage induced by water motion in the earth's magnetic field (Westerberg 1982b, 1984).

Supporting this mechanism was the change of the depth of salmon diving-excursions where a particular water mass changed its depth with a concomitant change in the salmon's swimming course (Westerberg 1982b). Further evidence for selection by salmon of a particular water stratum originating from its home stream is based upon chemical composition (Doving et al. 1985). Single olfactory bulb neurons responded differentially to water samples taken from those layers to which the salmon descended. Although this mechanism may be of use in finding the mouth of the home river, it may not be useful for guidance of salmon in the open ocean. Adult salmon with ablated olfactory nerves released at a river mouth returned to the home river almost as often as those with intact nerves (Hansen et al. 1987).

The vertical diving oscillations of the hammerheads were not restricted to crossing the strong thermal gradients and velocity shears in the transition zones between different water masses. Other oceanic fishes also do not restrict their oscillatory diving movements to the boundaries between different thermal gradients. For instance, this relationship was not apparent in depth records of eels (Fig. 9 of Tesch 1978) swordfish (Fig. 5 of Carey and Robison 1981), blue sharks (Fig. 1 of Carey and Scharold 1990), yellowfin and bigeye tunas (Holland et al. 1990b), and blue marlins (Holland et al. 1990a). However, restriction of up and down oscillations to the thermocline occurred in the white shark (Carey et al. 1982).

Geomagnetic field

Patterns of magnetization in the sea floor could be of potential benefit to oceanic animals as landmarks for guiding their movements. Magnetic minerals in the oceanic crust produce distortions in the relatively uniform north-south gradient to the earth's dipolar magnetic field, induced by circulation of conductive molten liquid in the outer core (Merrill and McElhinny 1983). Sea-floor magnetism is not measured directly, but is estimated at points as deviations (anomalies) from the measured total geomagnetic intensity after subtraction of a global dipolar component found by mathematically fitting a geocentric dipole to the distribution of intensity measurements on the surface of the earth (Skiles 1985). Departure from a simple north-south gradient (i.e., change over distance) of total field intensities is common, and this is more apparent on maps with small contour intervals and of fine spatial scale. These local distortions to the global dipole become larger with increasing water depth due to the disproportional increase in the contribution from the sea floor magnetization relative to that of the outer core.

Two magnetic patterns are particularly common on the sea floor. One pattern, evident at seamounts, is caused by the antiparallel alignment of magnetic particles extruded from the earth's core during different geological periods (Parker et al. 1987). The dipole field created around these seamounts could serve as a beacon to enable species to return to the seamount after foraging movements in the surrounding pelagic environment. Another pattern, ubiquitous to ocean basins, is alternating bands of weak and strong magnetization on either side of the spreading axis of two crustal plates (Skiles 1985). Steep intensity gradients exist between the bands which contain magnetic particles with dipole moments either parallel to or antiparallel to the present direction of the earth's dipole axis. The boundaries between the steep and weaker adjacent gradients could serve as geographic reference "roads" along which marine animals might migrate between temperate and tropical environments.

Evidence relating the movements of marine animals to patterns of sea floor magnetization is scant and contrary. Strandings of live cetaceans frequently occur at coastal points intersected by valleys in the local geomagnetic relief. It may be that the coast blocks the forward progress of cetaceans navigating along the bands of strong and weak magnetization (for coast of Britain, see Klinowska 1985; for northeast United States, see Kirschvink et al. 1986). However, straight-line movements by blue sharks off the northeast coast of North America did not always parallel contours of total field intensity, as would be expected were they orienting to that feature (Carey and Scharold 1990).

In the present study, the homing movements of sharks occurred along geographic paths that coincided with boundaries between different geomagnetic gradients. These boundaries were most obvious along ridges and valleys leading away from the seamount on the 3-D contour map of total geomagnetic intensity and the corresponding maxima and minima in the intensity trace produced by the magnetometer when towed around the seamount in concentric circles.

Klinowska (1985) reported that cetacean strandings occurred where valleys in the geomagnetic field intersected the coast of Great Britain or coastal islands. It is equally plausible that some of these strandings may have been from cetaceans swimming along the ridges of adjacent geomagnetic slopes. Kirschvink et al. (1986) compared stranding frequencies to the relative magnetic field along the coastline of the eastern United States. They concluded that cetaceans followed magnetic minima and avoided gradients. Their conclusion was based upon the high magnetic deviation (i.e., the difference of the mag-

netic field at the stranding site from the average intensity between maximum and minimum peak intensities) at increasing distances from the site. However, the lack of symmetry between the greater height of the peaks and lesser depth of the valleys relative to the entire record of magnetic intensities may have biased the result toward a relationship with minima and not maxima.

Hypothetical mechanism of orientation: geomagnetic topotaxis

The ability to orient to local maxima or minima in geomagnetic field intensity could be described as a geomagnetic *topotaxis*. The prefix *topo* describes the relationship of an animal's movement to topography – "the configuration of a surface including its relief and the position of its natural . . . features" (Gove 1966). The suffix *taxis* indicates that an animal is attracted to and actively tracks ridges and valleys, features of relief in a surface of geomagnetic field intensities.

It is essential to distinguish topotaxis from a compass-sense, i.e., the ability to maintain a heading using directional references such as sun, moon, stars, or earth's dipolar main field. These orientation mechanisms may best be distinguished from each other with an analogy to the quite different methods by which humans navigate large airplanes and helicopters. The airplane pilot navigates between two widely separated geographical points by steering in a direction relative to the northward orientation of the compass magnet, utilizing knowledge of the difference between the former direction and that of the destination, and returns by flying in a complementary direction. If the wind speed is strong and perpendicular to the plane's course, the airplane is deflected from the direction of the destination point, and the pilot changes course based upon knowledge of wind velocity to compensate for this deflection. The resulting flight path is often slightly curved. Similar paths are expected from an animal with a compass-sense. A helicopter, on the other hand, is often flown in relation to local features and, therefore, navigated differently. The helicopter pilot visually follows a road, valley, or ridge, resulting in a path that can be sinuous. The winding path of the helicopter depends upon that of the reference feature. Straight roads give straight flight paths, winding roads give winding paths.

Both elevational and geomagnetic topotaxis can result in complex paths relative to map contours. This is illustrated by visual navigation in which change in the steepness of the slope of the ground is used as a reference. Mountain ridges, valley bottoms, and edges of plateaus are easily followed by sight by animals with good vision. For instance, let us consider how human pioneers from the eastern United States crossed mountain ranges that lay perpendicular to their path to California. Using elevational topotaxis, they traveled a winding path beneath ridges at the base of steep slopes. Their reference was the change from the steep slope of the mountainside to the flat valley floor, and their track paralleled the closely-spaced contours of elevation indicating the steep slope of the mountain range. The same principle was used to cross mountain ranges. The best path was along the bottom of a canyon with the shallowest elevation gradient leading up the slope of the mountain range. Thus, on a contour map, the pioneer track crossed those elevation contours bending toward the ridge of the mountains with the most gradual elevation change. The path over the top of a ridge often followed a winding valley bottom with little elevation change parallel to elevation contours, and then led down a canyon on the other side. This example demonstrates how topotaxis, used as a travel strategy, will result in movements that both parallel and cross contours of elevation.

For this reason, topotaxis must not be rejected as a travel strategy just because the movements of an animal do not parallel contours of a particular intensity. An example of this was the movement of the three hammerheads near the seamount along Path 2 (stippled area in Fig. 8 B) across parallel, triangle-shaped contours indicating a small geomagnetic ravine leading from the seamount in a northern direction up and over a ridge. Although the triangles indicating the ravine on the 3-D contour map are small, the sides of the ravine are actually quite steep, as is evident from minimums in the magnetic intensity traces on Records A–D (Minimum 2, Fig. 10). The positions of the sharks during Tracks A1, B3, B4, and C5 coincided closely with the bottom of the minimum flanked on either side by steep slopes (Fig. 10 A–D).

This travel strategy may in part explain the absence of a strictly parallel relationship of the straight-line movements of blue sharks (*Prionace glauca*) tracked by Carey and Scharold (1990) with the 100 nT contours of total field intensity along the northeast coast of North America. The pattern of magnetic contours at the depth of these orienting sharks may have differed from that presented in the contour maps. In the survey of Klitgord and Behrendt (1979), the magnetometer was towed at a height of 450 m above ground where the magnetic intensity gradient would be considerably less steep than at the depths at which the sharks were swimming near the magnetized sea floor. Furthermore, the grid dimension of the aeromagnetic survey was 33×65 km much coarser than the 0.93×1.86-km grid dimension used in the present study, and the contour interval was 100 not 10 nT.

Elevation as a reference to guide human movements has been used to better understand the mechanism of topotaxis. The intensities of all physical properties vary over space, and any such property could form the basis for topotaxis. The intensity of the geomagnetic field over the earth's surface forms topographic features such as alternating ridges and valleys from magnetic reversal lineations and peaks from magnetic dipoles associated with seamounts. An ability to track such topographic relief would require that an animal possess some means of resolving minute geomagnetic intensity. For maximum discrimination, the animal's sensory receptors might be expected to be separated. The laterally enlarged rostrum of the hammerhead shark would be ideal for this purpose. The hammerhead could better identify the boundary between two gradients by a change in the intensity difference perceived between its widely separated receptors.

One sensory mechanism has already been suggested for geomagnetic orientation. This mechanism does not involve a topo-sense but a compass-sense. An animal could maintain a heading by avoiding any change in the electric field induced by a change in direction through the horizontal component of the earth's main field, termed "active electro-orientation" by Kalmijn (1984). Elasmobranchs possess receptors, the Ampullae of Lorenzini, that are sensitive to electric fields (Kalmijn 1966, 1982). A shark deriving only a heading relative to the axis of the dipole field, would drift with crosswise ocean currents, and would have difficulty maintaining a straight course. The course might be based upon the shark's ascertaining current speed and direction by detection of a voltage induced by the motion of salt water, a conductor, through the vertical component of the earth's main field, termed "passive electro-orientation" by Kalmijn (1984).

Although some tracks in the present study were in a single direction, easily explained by electro-orientation (Tracks A 1 and B 2 in Fig. 7 A, B), others consisted of parts with greatly different directions (Tracks B 4 and B 5 in Fig. 7 B, C). Such tracks are not easily explained by a compass-sense based upon electro-orientation. For example, the return and outward paths of Tracks B 4 and B 5 of Shark B were along an east-west axis near the seamount, along a north-south axis at an intermediate distance, and along an east-west axis again at greater distances from the seamount. With only a compass-sense, the shark would have to remember to turn in the proper direction to return to the seamount following its outward movement. The shark must change direction at a particular location after continuing farther eastward, reversing direction, swimming westward, and finally moving out and back along the north-south axis. This decision would be complicated by crosswise drift in the ocean current. Any adjustment by the shark must be based only upon the familiarity with the current velocities along its outward path. If the current changed direction prior to the shark's return, adjustment would be even more difficult. It is unlikely that the shark could make such adjustments solely using active and passive electro-orientation. Another possibility is that the shark turned upon recognizing the same geomagnetic ridge (Path 6 in Fig. 8 B and Fig. 10 A–D) that it had followed during its outward movement. An alternative explanation for the pattern of movement proposed here is that the shark possessed a topotaxis, orienting to boundaries between different geomagnetic gradients in sea-floor magnetization. Supporting this hypothesis is the fact that tracks often followed paths (heavy portions of tracks in Fig. 7) that coincided with maxima and minima in intensity traces on magnetometer records (Fig. 10) from ridges and valleys in the geomagnetic relief leading away from the seamount (Fig. 8 B).

What receptor might be used to perceive these minute geomagnetic gradients from the magnetization of the sea floor? Several receptor mechanisms have been proposed. Firstly, an electrical current is induced by an animal swimming through lines of magnetic force. This results in a voltage differential between the ampullae of Lorenzini located on either side of the shark's head. Sensory comparisons might not be made between single ampullae of Lorenzini, but instead between groups of receptors on either side of the shark's rostrum, leading to the dorsal roots of the left and right anterior lateral-line nerves (Northcutt 1978). Secondly, a differential in the exertion of a magnetic torque could exist between chains of ferrimagnetic particles such as magnetite in the shark's tissues (Kirschvink and Gould 1981). Although single-domain magnetite has yet to be detected in the tissues of elasmobranchs, chains of these particles have been detected in the tissues of salmon (Mann et al. 1988, Walker et al. 1988). Thirdly, a difference may exist between optical pumping of chemical compounds within the eyes (Leask 1977).

Based upon intensity change recorded per unit distance at the sea surface, the intensity differential across the hammerhead's rostrum would appear to be minute. However, an estimate based upon surface field-measurements is potentially misleading for a shark that swims at times at great depths (Klimley and Nelson 1984, Klimley 1993). At such depths, the geomagnetic intensity gradient may be much larger due to the greater contribution of the magnetization of the sea floor relative to that from the earth's core. In the present study, the geomagnetic intensity gradient measured for Shark A at a depth of 175 m was 0.0374 nT/m, almost three times the 0.0138 nT/m gradient at the surface. However, the magnitude of this gradient is smaller by a factor of 40 than the 1.2 nT/m gradient in magnetic intensity corresponding to the 5.0 nV/cm threshold of sensitivity determined for the round stingray (*Urolophus halleri*) by Kalmijn (1982). However, this threshold may not be representative of the hammerhead's magnetic sensory capability. The stingray may not have evolved a high degree of magnetic sensitivity because it does not inhabit the same environment as the hammerhead; in addition. The stingray has not been shown to possess the navigational ability of the scalloped hammerhead.

The magnitude of the subsurface gradient measured in the present study may be an underestimate of the true magnitude of the geomagnetic gradient at the position of the shark. Shark A was swimming along a tiny ridge between the western geomagnetic slope and eastern plateau (Peak 1, for Shark A in Fig. 10 D). Along the line drawn between Points A and B, the geomagnetic intensity increased to its maximum and then decreased again before the latter point. Unless Point B was exactly on Peak 1, the value calculated by dividing the intensity change over the distance between the two respective points would be based on a lower intensity and extra distance.

Geomagnetic gradient intensities are sufficiently large for the round stingray to detect at some depths. The intensity gradient at the sea surface and at an elevation of 100 m over a geomagnetic polarity reversal boundary were determined by Macdonald et al. (1980). At the surface, the geomagnetic anomaly intensity varied by 400 nT over a distance of 7 km; at 100 m above the sea floor, the anomaly intensity changed by 1400 nT over a distance of 1 km. The former gradient increased by a factor of 25 from 0.057 to 1.400 nT/m. The increase in intensity of local magnetic gradients with depth and their value in

guiding migration could be the reason for the oscillatory "yo-yo" diving pattern observed in hammerheads in the present study and in other species such as eels (Tesch 1978), swordfish (Carey and Robison 1981), salmon (Westerberg 1982b), blue sharks (Landesman 1984, Carey and Scharold 1990), marlin (Holland et al. 1990a), and tuna (Holland et al. 1990b).

Acknowledgements. Many United States and Mexican investigators participated in the arduous tracking activities carried out in this study. The former investigators consisted of S. Butler, H. Kent, K. Milligan, V. Welch, W. Strong, A. Stull, J. McKibben, P. Klimley, S. Mock, P. Nelson, K. Goldman, M. Kelly, B. Shaner, and L. Solis; the latter of E. Carreno, G. Ponce, J. Gosch, M. Ross, S. Bermejo, E. Goena, C. Alonso, A. Moehl, S. Lluch, E. Noltenius, P. Perez, and A. Tores. The official observers designated by the Mexican government during the three cruises to the Gulf of California were I. Cabrera, M. Roderiguez, and J. Castillo. C. Quantz assisted in plotting the telemetry tracks. An anonymous reviewer suggested the method of track simulation and other improvements to the manuscript. Support for the study was received from the Psychobiology, Biological Oceanography and Oceanographic Technology Programs of the National Science Foundation through Grants BNS-84-19076, BNS-87-08304, and OCE-92-23808.

Literature cited

Bovet, P., Benhamou, S. (1988). Spatial analysis of animals' movements using a correlated random walk model. J. theor. Biol. 131: 419–433

Carey, F. G., Kanwisher, J. W., Brazier, O., Gabrielson, G., Casey, J. G., Pratt, Jr., H. L. (1982). Temperature and activities of a white shark, *Carcharodon carcharias*. Copeia 1982: 254–260

Carey, F. G., Robison, B. H. (1981). Daily patterns in the activities of swordfish, *Xiphias gladius*, observed by acoustic telemetry. Fish. Bull. U.S. 79: 277–292

Carey, F. G., Scharold, J. V. (1990). Movements of blue sharks (*Prionace glauca*) in depth and course. Mar. Biol. 106: 329–342

Cigas, J., Klimley, A. P. (1987). A microcomputer interface for decoding telemetry data and displaying them numerically and graphically in real time. Behav. Res. Meth., Instrums, Computers 19: 19–25

Doving, K. B., Westerberg, H., Johnsen, P. B. (1985). Role of olfaction in the behavioral and neuronal responses of Atlantic salmon, *Salmo salar*, to hydrographic stratification. Can. J. Fish. aquat. Sciences 42: 1658–1667

Gove, P. B. (ed.) (1966). Webster's third new international dictionary of the English language. G & C Merriam Co., Springfield, Mass.

Greer Walker, M., Harden Jones, F. R., Arnold, G. P. (1978). The movements of plaice (*Pleuronectes platessa* L.) tracked in the open sea. J. Cons. int. Explor. Mer. 38: 58–86

Gruber, S. H. (1967). A behavioral measurement of dark adaptation in the lemon shark, *Negaprion brevirostris*. In: Gilbert, P. W., Mathewson, R. F., Rall, D. P. (eds.) Sharks, skates and rays. Johns Hopkins Press, Balitmore, p. 479–490

Gruber, S. H., Cohen, J. L. (1978). Visual system of the elasmobranchs: state of the art 1960–1975. In: Hodgson, E. S., Mathewson, R. F. (eds.) Sensory biology of sharks, skates and rays. U.S. Government Printing Office, Washington, p. 11–105

Gruber, S. H., Nelson, D. R., Morrissey, J. F. (1988). Patterns of activity and space utilization of lemon sharks, *Negaprion brevirostris*, in a shallow Bahamian lagoon. Bull. mar. Sci. 43: 61–76

Hansen, L. P., Doving, K. B., Jonsson, B. (1987). Migration of farmed adult Atlantic salmon with and without olfactory sense, released on the Norwegian coast. J. Fish Biol. 30: 713–721

Harden Jones, F. R. (1981). Fish migration: strategy and tactics. In: Aidley, D. J. (ed.) Animal migration. Cambridge University Press, Cambridge, p. 139–165

Harden Jones, F. R., Arnold, G. P. (1982). Acoustic telemetry and the marine fisheries. In: Cheeseman, C. L., Mitson, R. B. (eds.) Telemetry studies of vertebrates. Academic Press, London, p. 75–93

Hawryshyn, C. W., Arnold, M. G., Browning, E., Cole, R. C. (1990). Spatial orientation of rainbow trout to plane-polarized light: the ontogeny of E-vector discrimination and spectral sensitivity characteristics. J. comp. Physiol. (Sect. A) 166: 565–574

Hawryshyn, C. W., McFarland, W. N. (1987). Cone photoreceptor mechanisms and the detection of polarized light in fish. J. comp. Physiol. (Sect. A) 160: 459–465

Hiramatsu, K., Ishida, Y. (1989). Random movement and orientation in pink salmon (*Oncorhynchus gorbuscha*) migrations. Can. J. Fish. aquat. Sciences 46: 1062–1066

Holland, K., Brill, R. W., Chang, R. K. C. (1990a). Horizontal and vertical movements of Pacific blue marlin captured and released using sportfishing gear. Fish. Bull. U.S. 88: 397–402

Holland, K., Brill, R. W., Chang, R. K. C. (1990b). Horizontal and vertical movements of yellowfin and bigeye tuna associated with fish aggregating devices. Fish. Bull. U.S. 88: 493–507

Hurn, J. (1989). GPS. Trimble Navigation, Sunnyvale, California

Jamon, M. (1990). A reassessment of the random hypothesis in the ocean migration of Pacific salmon. J. theor. Biol. 143: 197–213

Kalmijn, A. J. (1966). Electro-perception in sharks and rays. Nature, Lond. 212: 1232–1233

Kalmijn, A. J. (1982). Electric and magnetic field detection in elasmobranch fishes. Science, N.Y. 318: 916–918

Kalmijn, A. J. (1984). Theory of electromagnetic orientation: a further analysis. In: Bolis, L., Keynes, R. D., Maddrell, S. H. P. (eds.) Physiology of sensory systems. Cambridge University Press, London, p. 525–560

Kirschvink, J. L., Dizon, A. E., Westphal, J. A. (1986). Evidence from strandings for geomagnetic sensitivity in cetaceans. J. exp. Biol. 120: 1–24

Kirschvink, J. L., Gould, J. L. (1981). Biogenic magnetite as a basis for magnetic sensitivity in animals. Biosystems 13: 181–201

Klimley, A. P. (1985). Schooling in *Sphyrna lewini*, a species with low risk of predation: a non-egalitarian state. Z. Tierpsychol. 70: 297–319

Klimley, A. P. (1987). The determinants of sexual segregation in the scalloped hammerhead shark, *Sphyrna lewini*. Envir. Biol. Fish. 18: 27–40

Klimley, A. P., Butler, S. B., Nelson, D. R., Stull, A. T. (1988). Diel movements of scalloped hammerhead sharks, *Sphyrna lewini* Griffith and Smith, to and from a seamount in the Gulf of California. J. Fish Biol. 33: 751–761

Klimley, A. P., Cabrera-Mancilla, I., Castillo-Geniz, J. L. (1993). Horizontal and vertical movements of the scalloped hammerhead shark, *Sphyrna lewini*, in the Southern Gulf of California, Mexico. Ciencias mar. 19: 95–115

Klimley, A. P., Nelson, D. R. (1984). Diel movement patterns of the scalloped hammerhead shark (*Sphyrna lewini*) in relation to El Bajo Espiritu Santo: a refuging central-position system. Behavl Ecol. Sociobiol. 15: 45–54

Klinowska, M. (1985). Cetacean live stranding sites relate to geomagnetic topography. Aquat. Mammals 1: 27–32

Klitgord, K. M., Behrendt, J. C. (1979). Basic structure of the U.S. Atlantic margin. Mem. Am. Ass. Petrol. Geol. 29: 85–112

Landesman, J. G. (1984). Horizontal and vertical movements and seasonal population shifts in the blue shark, *Prionace glauca*, near Santa Catalina Island. thesis. California State University, Long Beach, California

Leask, M. J. M. (1977). A physiochemico mechanism for magnetic field detection by migratory birds and homing pigeons. Nature, Lond. 267: 144–145

Macdonald, K. C., Miller, S. P., Huestis, S. P., Spiess, F. N. (1980). Three-dimensional modeling of a magnetic reversal boundary from inversion of deep-tow measurements. J. geophys. Res. 85: 3670–3680

Mann, S., Sparks, N. H., Walker, M. M., Kirschvink, J. L. (1988). Ultrastructure morphology and organization of biogenic mag-

netite from sockeye salmon, *Onchorhynchus nerka*: implications for magnetoreception. J. exp. Biol. 140: 35–49
McFarland, W. N. (1991). Light in the sea: the optical world of elasmobranchs. J. exp. Zool. (Suppl.) 5: 3–12
Merrill, R. T., McElhinny, M. W. (1983). The earth's magnetic field. Academic Press, London
Mitson, R. B., Storeton West, T. J., Pearson, N. D. (1982). Trials of an acoustic transponding fish tag compass. Biotelemetry Patient Monitg 9: 69–79
Northcutt, R. G. (1978). Brain organization in the cartilaginous fishes. In: Hodgson, E. H., Mathewson, R. F. (eds.) Sensory biology of sharks, skates, and rays. Government Printing Office, Washington D. C., p. 107–193
O'Gower, A. K., Mathewson, R. F. (1967). Spectral sensitivity and flicker fusion frequency of the lemon shark, *Negaprion brevirostris*. In: Gilbert, P. W., Mathewson, R. F., Rall, D. P. (eds.) Sharks, skates and rays, Johns Hopkins Press, Baltimore, p. 433–446
Parker, R. L., Shure, L., Hildebrand, J. A. (1987). The application of inverse theory to seamount magnetism. Rev. Geophys. 25: 1–65
Rohlf, F. J., Sokal, R. P. (1969). Statistical tables. W. H. Freeman & Company, San Francisco
Quinn, T. P., Groot, C. (1984). Pacific salmon (*Onchorhynchus*) migrations: orientation versus random movement. Can. J. Fish. aquat. Sciences 41: 1319–1324
Quinn, T. P., Terhune, B. A., Groot, C. (1989). Migratory orientation and vertical movements of homing adult sockeye salmon, *Oncorhynchus nerka*, in coastal waters. Anim. Behav. 37: 587–599
Saila, S. B., Shappy, R. A. (1963). Random movement and orientation in salmon migration. J. Cons. perm. int. Explor. Mer 28: 155–166
Skiles, D. D. (1985). The geomagnetic field: its nature, history, and biological relevance. In: Kirschvink, J. L., Jones, D. S., MacFadden, B. J. (eds.) Magnetite biomineralization and magnetoreception in organisms. Plenum Press, New York, p. 43–102
Tesch, F. W. (1978). Horizontal and vertical swimming of eels during the spawning migration at the edge of the continental shelf. In: Schmidt-Koenig, K., Keeton, W. T. (eds.) Animal migration, navigation, and homing. Springer-Verlag, Berlin, p. 378–391
Walcott, C., Lednor, A. J. (1983). Bird navigation. In: Brush, A. H., Clark, Jr., G. A. (eds.) Perspectives in ornithology. Cambridge University Press, Cambridge, p. 511–549
Walker, M. M., Quinn, T. P., Kirschvink, J. L., Groot, C. (1988). Production of single-domain magnetite throughout life by sockeye salmon, *Onchorhynchus nerka*. J. exp. Biol. 140: 51–63
Waterman, T. H., Forward, R. B. (1972). Field demonstration of polarotaxis in the fish *Zenarchopterus*. J. exp. Zool. 180: 33–54
Westerberg, H. (1982a). Ultrasonic tracking of Atlantic salmon (*Salmo salar* L.). I. Movements in coastal regions. Rep. Inst. Freshwat. Res. Drottningholm 60: 81–101
Westerberg, H. (1982b). Ultrasonic tracking of Atlantic salmon (*Salmo salar* L.). II. Swimming depth and temperature stratification. Rep. Inst. Freshwat. Res. Drottningholm 60: 102–120
Westerberg, H. (1984). The orientation of fish and the vertical stratification at fine- and micro-structure scales. In: McCleave, J. D., Arnold, G. P., Dodson, J. J., Neill, W. H. (eds.) Mechanisms of migration in fishes. Plenum Press, New York, p. 179–203
Winn, H. W., Salmon, M., Roberts, N. (1964). Sun-compass orientation by parrot fishes. Z. Tierpsychol. 21: 798–812
Zar, J. H. (1974). Biostatistical analysis. Prentice-Hall, Englewood Cliffs, Jersey

Communicated by M. G. Hadfield, Honolulu